Advances in performance of nitrate salts-based phase change materials and casing heat accumulator: A comprehensive review

Shang Mao[a,b,1], Kaile Hao[a,1], Xuehong Wu[a,b,*], Yong Liu[a,b], Shuang Cao[a,b], Yanping Du[c*]

a. *School of Energy and Power Engineering, Zhengzhou University of Light Industry, 450002, People's Republic of China*

b. *Henan International Joint Laboratory of Energy Efficient Conversion and Utilization, Zhengzhou University of Light Industry, 450002, People's Republic of China*

c. *School of Engineering, Lancaster University, Lancaster LA14YW, UK*

Abstract:

The key to improving the energy storage efficiency of solar thermal storage systems lies in developing high-performance thermal storage materials and optimizing the structure of thermal storage devices to address the technical challenges posed by the intermittent and unstable nature of solar radiation. Currently, nitrates salt phase change materials (PCMs) are widely used in solar thermal power generation systems, however, conventional molten salts suffer from limitations such as a narrow operating temperature range and poor thermal conductivity. Thermal storage devices, meanwhile, face challenges including limited optimization options and low thermal storage efficiency. To address these issues, this paper summarized the preparation of modified nitrates and the performance optimization of casing

[1] Authors contributed equally to this work.

*Corresponding author: *E-mail address:* wuxh1212@163.com (X. Wu); y.du17@lancaster.ac.uk

heat accumulators. The performance of single and mixed nitrates was compared and methods for improving performance were analyzed. Subsequently, the optimization of casing heat accumulator structures is examined, focusing on tube geometries, fin configurations, topology optimization and biomimetic design. Moreover, the synergistic optimization between nitrate-based PCMs and casing heat accumulators was proposed. Finally, the critical challenges and promising future research directions were prospected from nitrate-based PCMs development and heat accumulator optimization perspectives.

Keywords: Nitrate phase change material; Casing heat accumulator; Thermophysical property improvement; Heat accumulator optimization; Solar thermal storage

Nomenclature

Symbols		Fe_2O_3	iron oxide
c_p	specific heat capacity, J/(kg·K)	GA	graphene aerogel
ΔH	fusion enthalpy, J/g	GNS	graphene nanosheets
T	temperature, K	GO	graphene oxide
Greek symbols		HTF	heat transfer fluid
λ	thermal conductivity, W/(m·K)	MgO	magnesium oxide
ρ	density, kg/m^3	SiO_2	silicon dioxide
Subscripts		TiO_2	titanium oxide
m	melting point	LHTES	latent heat thermal energy storage
d	decomposition temperature	MWCNTs	multi-walled carbon nanotubes
Abbreviations		$NaNO_3$	Sodium nitrate

Al_2O_3	Aluminum oxide	PCMs	Phase change materials
CNTs	carbon nanotubes	SWCNTs	Single-walled carbon nanotubes
CSP	Concentrated solar power	TES	Thermal energy storage
CuO	copper oxide	TNC	ternary nitrate-carbonate
EG	expanded graphite		

1 Introduction

Industrial development has long been a cornerstone of national economic growth and social progress, with advancements in technology serving as a key driver of modernization [1]. In this context, the efficiency of energy utilization and innovation mode directly affect the competitiveness of industry and the sustainable development of the country. Since the Industrial Revolution, fossil energy as the dominant energy source has driven the rapid development of global industrialization. However, with the continuous increase in global energy demand, the depletion of conventional fossil fuels and the intensification of environmental pollution have become increasingly serious issues, driving a global shift toward clean and renewable energy sources [2]. Clean energy technologies such as solar thermal power, wind, photovoltaic, hydrogen and fourth-generation nuclear energy have become the critical directions for energy transformation [3].

Solar energy has been widely used in photovoltaic and solar thermal power generation due to the short life cycle, low cost and low carbon emissions [4]. Although Chinese solar power capacity has grown rapidly in recent years, the inherent intermittency and volatility of solar

power have limited its stable grid integration. Efficient thermal energy storage (TES) technology has become the key to overcoming this bottleneck [5]. TES technologies enable the storage of excess energy during periods of low demand and its release during peak demand, thereby significantly enhancing overall energy utilization efficiency and facilitating the large-scale deployment of renewable energy systems. Concentrated solar power (CSP) systems, relying on molten salt thermal storage technology to achieve all-weather stable power generation [6], have become a key direction of renewable energy development, with higher operational stability and peak-shaving capacity than photovoltaic power generation [7]. Among various TES technologies, phase change materials (PCMs) have become a key solution to address solar energy fluctuations due to high energy storage density and reversible phase change characteristics [8]. In the mid-to-high temperature range, typically 120-500 ℃, which is particularly relevant for CSP and industrial waste heat recovery, molten salt PCMs exhibit unique and irreplaceable advantages. Compared with other PCM candidates, molten salts offer excellent thermal stability, high latent heat, wide availability and low cost [9]. Notably, nitrate-based molten salts stand out due to their favorable melting temperature range, low corrosivity, and superior thermal stability, making them among the most promising TES materials for CSP applications. Despite these advantages, their practical deployment is constrained by inherent limitations, including relatively low thermal conductivity and a narrow operating temperature window, which hinder efficient heat transfer and system responsiveness [10].

The heat accumulator is the core component of an integrated PCM system and its performance directly determines the overall efficiency and economic viability of the TES

system [11]. Conventional accumulator designs often suffer from uneven heat flow distribution, slow melting rates, and incomplete phase change, which can lead to localized overheating, material corrosion, and salt decomposition, ultimately shortening equipment lifespan [12]. Rational design of rib structures and heat exchange surfaces can significantly improve heat transfer efficiency and boost the effectiveness of the thermal energy storage system. [13]. These issues have become key obstacles hindering the large-scale engineering application of nitrate-based PCM TES technology in solar thermal power generation. Therefore, optimization of nitrate-based PCM and heat accumulator is crucial for improving system performance.

To address the limitations of nitrate-based PCMs and their associated heat accumulators, this review systematically synthesizes recent advances in material modification and structural optimization, with a particular focus on casing heat accumulator. Unlike previous reviews that have addressed material development or heat exchanger design separately, this work presents a holistic integration of material-structure-performance strategies. Specifically, we summarize advanced approaches for enhancing nitrate PCMs, including mixed molten salt formulations and thermal conductivity improvement techniques. We further discuss various optimization strategies for casing heat accumulators, such as fin configurations and heat surface modifications, providing practical guidance for integrated system design. The optimization strategies for hybrid nitrate PCMs, thermophysical enhancements and practical applications, are illustrated in Fig. 1. Finally, we identify key challenges and future research directions for the synergistic optimization of nitrate-based PCMs and casing heat accumulator. Overall, this

review aims to advance the development and application of nitrate-based PCMs and their coupled accumulator systems in the field of solar thermal energy storage.

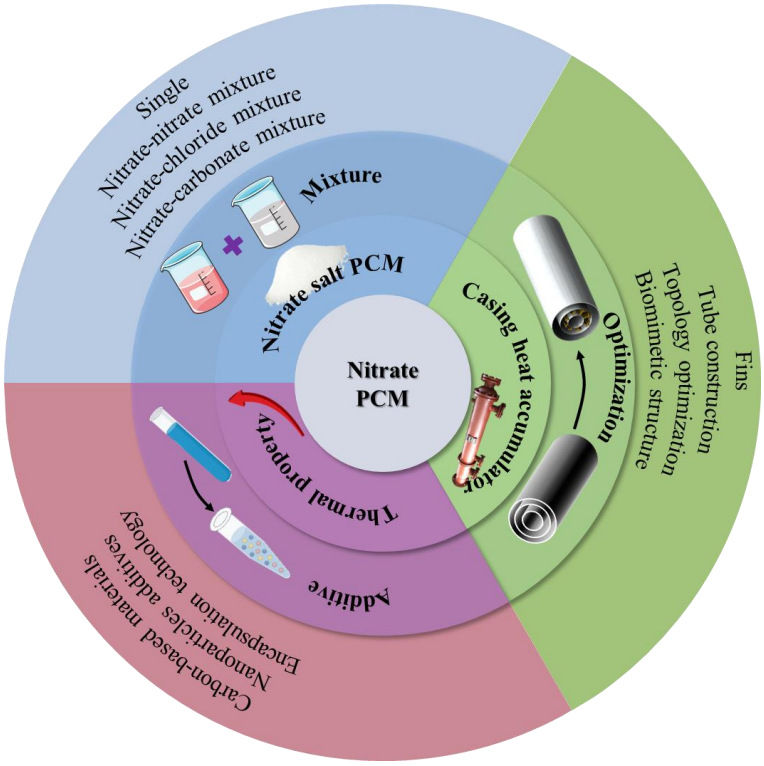

Fig. 1. Performance improvement of molten salt and casing heat accumulator.

2 Nitrate molten salt PCMs

PCM plays an important role in phase change heat storage in industrial and civil applications [14] and can be categorized according to the form of phase change, temperature range and chemical components. They can be categorized into three types according to the temperature range: low temperature (-50~100 ℃), medium temperature (100~250 ℃) and high temperature (above 250 ℃) [15]. Low-temperature PCM, such as hydrogels and inorganic hydrated salts, are mainly used in construction [16]. Medium-temperature PCM, like molten salts and polymers, are widely used in the field of construction and solar energy [17]. High-temperature PCM, such as molten salts, metals and alloys, are mainly used in industrial waste

heat recovery and power peaking [18]. With the growing demand for energy-efficient technologies, the application of phase change materials (PCMs) is expanding, particularly in the field of solar energy, where their thermal storage performance directly impacts overall system efficiency.

2.1 Single nitrates utilized for solar energy

In solar energy utilization, concentrated solar power (CSP) systems impose particularly stringent requirements on thermal storage media, which must balance thermal stability, temperature adaptability, and cost-effectiveness. Therefore, the selection of appropriate thermal storage materials is critical for the design and operation of CSP systems. Molten salts have emerged as one of the preferred choices due to their excellent thermal stability, high heat storage density, and wide operational temperature range [19]. The improvement of the efficiency and stability of CSP systems relies on in-depth studies of the thermophysical properties of molten salts. Molten salts include nitrates, carbonates and chlorides [20], among which nitrate materials have the advantages of relatively low melting points (usually below 300 ℃), moderate heat capacity and good chemical stability. Carbonates and chlorinated salts perform well in environments above 400 ℃ and have potential application in high temperature systems. According to the chemical composition, the classification of molten salt PCM suitable for CSP is listed in Table 1. Compared to conventional high-temperature molten salts, low and medium-temperature molten salt systems are able to operate at lower temperatures, reducing energy consumption and improving energy utilization efficiency, saving energy costs. Therefore, nitrate-based materials are considered the optimal choice for low- to medium-temperature CSP

systems. Their phase transition temperatures range from 300 to 550 ℃ aligning well with the typical operating ranges of trough (300–400 ℃) and tower (500–550 ℃) CSP systems, without the need for additional heating or cooling. The thermophysical properties of individual nitrate salts are summarized in Table 2.

Table 1. Classification of molten salt PCM for CSP.

Molten salt type	T_m (℃)	Advantages and disadvantages
Nitrates	200-600	High latent heat of phase change, Chemically stable, Low cost, Non-toxic, Good liquidity Less corrosive
Chlorides	400-800	Good high-temperature stability, High thermal conductivity, Easy to absorb moisture, Strong corrosiveness, High cost
Carbonates	400-800	Good high-temperature stability, Low latent heat of phase change, Easy to react with water, Poor liquidity
Fluorides	600-1000	High temperature resistance, High toxicity, Extremely high cost, Extremely corrosive, Poor safety

Table 2. Thermal-physical properties of single nitrate salts.

Nitrates	T_m (℃)	T_d (℃)	ΔH (J/g)	Ref.

KNO_3	336.9	400	95	[21]
$NaNO_3$	309.08	380	165.25	[22]
$Ca(NO_3)_2$	561	561-660	145	[23]
$LiNO_3$	264	600	360	[23]
$NaNO_2$	270	320	180	[23]
$Ba(NO_3)_2$	561	592	145	[23]
$Sr(NO_3)_2$	608	645	221	[23]
$Mg(NO_3)_2$	129	330	189	[24]

2.2 Nitrate-nitrate mixture

Solar Salt (60% $NaNO_3$-40% KNO_3) has a melting point of 220 ℃ and Hitec salt (53% KNO_3-40% $NaNO_2$-7% $NaNO_3$) melts at 142 ℃ [25]. The phase transition temperature of mixed nitrate salts can be flexibly adjusted by varying the component ratios, making them suitable for most medium and high temperature thermal energy storage applications. Solidification can be effectively prevented through heat tracing and insulation, enabling large-scale pipeline transport and storage tank design. The long-term reliability of these salts has been demonstrated in multiple commercial CSP power plants worldwide [26, 27]. Mixed nitrate salts can be classified into binary, ternary, quaternary, and multinary mixtures based on the number of components they contain, as shown in Fig. 2.

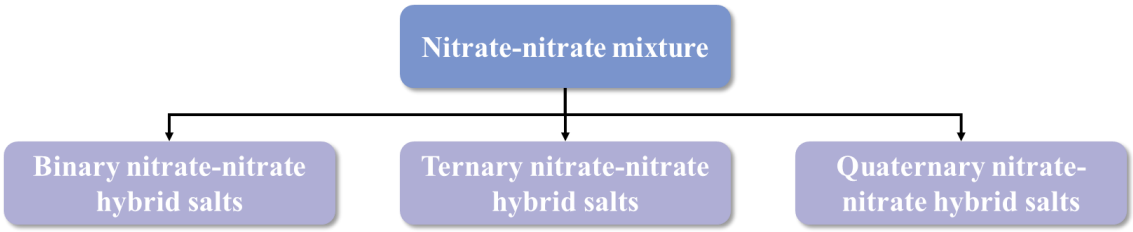

Fig. 2. Classifications of nitrate-nitrate mixture.

2.2.1 *Binary nitrate-nitrate hybrid salts*

The introduction of other nitrates to the molten salt can alter the properties of the single nitrate. Solar salt containing 40% KNO_3 and 60% $NaNO_3$ is commonly used binary nitrate molten salts due to their suitable melting point and high decomposition temperature [28]. Wang et al. [29] focused on 50% $NaNO_3$-50% KNO_2 and 44% $NaNO_3$-56% $NaNO_2$ binary nitrate/nitrite molten salts, and predicted the thermal properties of mixed molten salts through machine learning and phase diagrams. Wang et al. [30] investigated various binary nitrate molten salts, including $NaNO_3$-KNO_3, $NaNO_3$-$LiNO_3$, KNO_3-$LiNO_3$, KNO_3-$Ca(NO_3)_2$, $LiNO_3$-$Ca(NO_3)_2$ and $NaNO_3$-$Ca(NO_3)_2$. The melting points (T_m) of these binary nitrate salts ranged from 136.7 ℃ to 239.2 ℃. The common binary nitrate-nitrate hybrid salt is shown in Table. 3. Some binary nitrate molten salts have high decomposition temperatures and can operate stably at elevated temperatures. For example, the decomposition temperature of 50% $NaNO_3$-50% KNO_2 was 642.2 ℃, which could meet certain high-temperature application requirements. By adjusting the component ratios, certain binary nitrate molten salts can achieve lower melting points, which helps reduce energy consumption during system start-up and operation while preventing solidification. For example, the melting point of 50% $NaNO_3$-50% KNO_2 is 139.1 ℃, which is lower than the single nitrates. Moreover, binary molten salts based

on $NaNO_3$ and KNO_3 have relatively low raw material costs and are suitable for large-scale application. However, binary molten salts containing nitrite ions (NO_2^-) may exhibit some corrosion potential toward metals at high temperatures, potentially affecting the service life of system equipment. The phase transition behavior of binary nitrate molten salts may exhibit irregularities, potentially affecting the stability of energy storage and release. Although a variety of binary nitrate compositions have been developed, comprehensive data on their decomposition temperatures (T_d) and fusion enthalpy (ΔH) remain limited. Further refinement of these thermophysical properties is necessary to provide reliable technical data for practical applications. Clearly, the melting point can be significantly lowered by adding KNO_2 or $LiNO_3$, reaching as low as 136.7 ℃, whereas the melting point of binary nitrate mixtures containing $Ca(NO_3)_2$ is typically above 220 ℃. The decomposition temperature of binary mixtures containing nitrite is slightly higher than that of Solar salt, but the latent heat is significantly lower. Consequently, binary systems containing $LiNO_3$ offer significant advantages in terms of melting point, addressing the issues of pipe blockages and high energy consumption for system insulation associated with traditional molten salts.

Table. 3. Summary of binary nitrate-nitrate hybrid salts.

Component	T_m (℃)	T_d (℃)	ΔH (J/g)	Ref.
60% $NaNO_3$-40% KNO_3 (Solar salt)	220.0	600.0	161	[28]
50% $NaNO_3$-50% KNO_2	139.1	642.2	74.7	[29]
44% $NaNO_3$-56% $NaNO_2$	222.0	632.0	121.2	[29]
48.9% $NaNO_3$-51.1% KNO_3	224.3	-	-	[30]

48.4% $NaNO_3$-51.6% $LiNO_3$	196.7	-	-	[30]
57.5% KNO_3-42.5% $LiNO_3$	136.7	-	-	[30]
67% KNO_3-33%$Ca(NO_3)_2$	148.3	-	-	[30]
86.3% $LiNO_3$-13.7% $Ca(NO_3)_2$	239.3	-	-	[30]
67.7% $NaNO_3$-32.3% $Ca(NO_3)_2$	224.3	-	-	[30]

2.2.2 *Ternary nitrate-nitrate hybrid salts*

Compared to conventional Solar Salts, ternary molten salts based on $NaNO_3$ and KNO_3 can further enhance key performance characteristics. The addition of a third nitrate component, such as Li NO_3 or $Ca(NO_3)_2$, preserves the high thermal storage density and chemical stability of the molten salts while maintaining relatively low cost. Hitec salt, a ternary mixture consisting of 7% $NaNO_3$, $NaNO_2$, and 53% KNO_3, features a low melting point (142 °C), high decomposition temperature (T_d 535 ℃), low cost, and non-toxic properties, making it widely adopted in CSP systems [31]. Olivares et al. [32] studied the thermal stability of a ternary nitrate composed of 30% $LiNO_3$-18% $NaNO_3$-52% KNO_3 and determined the applicable temperature (121 ℃) and enthalpy value (141.2 J/g) for TES. Recently, Fernández et al. [33] studied the effect of adding $LiNO_3$ and $Ca(NO_3)_2$ to Solar Salt on physical and chemical properties. The results showed that the addition of $LiNO_3$ improved the thermal stability of the salt, while the addition of $Ca(NO_3)_2$ lowered the T_m. Li et al. [34] investigated the degradation mechanism of the thermal-physical properties of a ternary molten salt composed of 16% $NaNO_3$-48% KNO_3-36% $Ca(NO_3)_2$ after long-term high-temperature heat treatment. The results showed that the T_m decreased from 103.3 ℃ to 98.3 ℃ and the ΔH increased from 28.83 J/g to 32.45 J/g after 15

days of high-temperature treatment at 480.0 ℃. Zhao et al. [35] developed a ternary nitrate mixtures composed of 63.7% KNO_3-27.3% $Ca(NO_3)_2$-9% $LiNO_3$ and the results showed that the mixtures have a T_m of 100 ℃ and high T_d of 500 ℃. The detailed information of ternary nitrate is listed in Table. 4. Henríquez et al. [36] reported that the T_m of 30% $LiNO_3$-13% $NaNO_3$-57% KNO_3 was 124 ℃ and the T_d was 594 ℃, which meant that the mixture could operate at the highest operating temperature similar to that of Solar Salts. It can be seen that ternary nitrates have lower T_m, which can effectively broaden the operating temperature range and reduce the risk of system freezing. Compared with binary salts, ternary salts can further lower the melting point and are generally much lower than binary Solar Salts. The nitrite-based system exhibits the best thermal stability, with a decomposition temperature as high as 652 ℃. $LiNO_3$-based ternary systems are the primary focus for medium-temperature TES. They combine the advantages of low melting points and high phase-change enthalpy, offering TES densities close to those of traditional Solar Salt while featuring lower melting points, achieving the best overall performance. However, the relatively high cost of $LiNO_3$ makes ternary mixtures containing this component less competitive compared to conventional Solar Salts. Therefore, both the performance benefits and material costs of ternary nitrates should be carefully considered in future research and system design.

Table. 4. Summary of ternary nitrate-nitrate hybrid salts.

Component	T_m (℃)	T_d (℃)	ΔH (J/g)	Ref.
53% KNO_3-40% $NaNO_2$-7% $NaNO_3$(Hitec salt)	142.0	610.0	72.5	[25]
30% $LiNO_3$-18% $NaNO_3$-52% KNO_3	141.2	602	141.2	[32]

32.4% $Ca(NO_3)_2$-12.4% $NaNO_3$-55.2% KNO_3	115.6	500.0	-	[37]
48% $Ca(NO_3)_2$-7% $NaNO_3$-45% KNO_3	130.6	554.4	-	[38]
20% $LiNO_3$-52% KNO_3-28% $NaNO_3$	130.2	600.1	-	[38]
30% $LiNO_3$-60% KNO_3-10% $Ca(NO_3)_2$	132.2	567.1	-	[38]
42% KNO_3-48.5% $NaNO_2$-9.5% KNO_2	139.8	652.0	-	[33]
40% $NaNO_2$-7% $NaNO_3$-53% KNO_3	142.0	631.0	-	[39]

2.2.3 *Quaternary nitrate-nitrate hybrid salts*

Although binary and ternary nitrate molten salts such as Solar Salts and Li-containing ternary salts have been extensively investigated, practical applications still face challenges including high melting points, limited high-temperature stability, and elevated costs. To address these issues, quaternary nitrate salts, which incorporate a fourth nitrate component into ternary systems, have been developed. These quaternary mixtures exhibit lower melting points, as summarized in Table. 5. Fernández et al. [40] proposed a quaternary nitrate containing $LiNO_3$ and Ca $(NO_3)_2$ to improve the solar salt used in CSP, extending the operating temperature range to 132-580 ℃. Zhong et al. [24] conducted thermodynamic calculations on quaternary 11.3% $Mg(NO_3)_2$-20.7% $LiNO_3$-56.4% KNO_3-11.6% $NaNO_3$ with the aim of designing a new type of $Mg(NO_3)_2$ based molten salt with a low melting point, which had T_m=116.9 ℃ and T_d=473.2 ℃, ΔH=133.7 J/g. Gasanaliev et al. [41] proposed a quaternary salt consisting of 29% $LiNO_3$-17% $NaNO_3$-49.4% KNO_3-4.6% $Sr(NO_3)_2$, which had a high ΔH=229.6 J/g. Moreover, Mantha et al. [42] developed a new model based on thermodynamic principles to predict the thermal parameters of 17.5% $LiNO_3$-14.2% $NaNO_3$-50.5% KNO_3-17.8%$NaNO_2$. The results showed

that T_m=99.8 ℃, ΔH=16.8 J/g. Iverson et al. [43] developed quaternary nitrates with T_m below 100 ℃ to reduce the risk of molten salt solidification. Zou et al. [44] improved the thermal properties of Hitec salt by introducing $Ca(NO_3)_2$ and conducted long-term and cyclic thermal stability tests. The results showed that the molten salt had a low T_m=83.1 ℃ and a high T_d=628.5 ℃, making it suitable as a heat transfer and heat storage medium for CSP systems. Kwasi-Effah et al. [45] developed and characterized a novel quaternary nitrate molten salt mixture and investigated the effect of $LiNO_3$ on thermal properties. The results showed that T_m decreased with increasing $LiNO_3$, with the lowest T_m=73.5 ℃ at a $LiNO_3$ mass content of 35%. As the ratio of $LiNO_3$ to $Ca(NO_3)_2$ increases and $NaNO_2$ is introduced, the T_m of the mixed nitrates shows a significant downward trend, decreasing from 132.1 ℃ to 73.5 ℃. The low T_m can reduce the risk of pipe freezing and lower insulation energy consumption during winter or at night, making them particularly suitable for applications with high requirements for low-temperature fluidity, such as parabolic trough solar power plants. Unfortunately, decomposition temperatures or enthalpies of phase transition are unavailable for most quaternary systems, posing a key obstacle to engineering applications. Future research should systematically test the thermal properties of quaternary systems with different compositions to clarify the regulatory mechanisms of component ratios on melting point, decomposition temperature and phase transition enthalpy, providing data support for the precise selection of thermal storage media in solar thermal power generation.

Table. 5. Summary of quaternary nitrate-nitrate hybrid salts.

Component	T_m (℃)	T_d (℃)	ΔH (J/g)	Ref.

10% $LiNO_3$-20% $NaNO_3$-60% KNO_3-10% $Ca(NO_3)_2$	132.1	580.4	-	[40]
29% $LiNO_3$-17% $NaNO_3$-49.4% KNO_3-4.6% $Sr(NO_3)_2$	105	-	229.6	[41]
11.3% $Mg(NO_3)_2$-20.7% $LiNO_3$-56.4% KNO_3-11.6% $NaNO_3$	116.9	473.2	133.7	[24]
17.5% $LiNO_3$-14.2% $NaNO_3$-50.5% KNO_3-17.8%$NaNO_2$.	99.8	-	16.8	[42]
42.3% KNO_3-39.4% $Ca(NO_3)_2$-12.1% $NaNO_3$-6.1% $LiNO_3$	90	-	15.2	[43]
16.7% Ca $(NO_3)_2$-44.2% KNO_3-5.8% $NaNO_3$-33.3% $NaNO_2$	83.1	628.5	71.75	[44]
28% $Ca(NO_3)_2$-35% $LiNO_3$-18% KNO_3 -19% $NaNO_2$	73.5	620	-	[45]

2.3 Nitrate-chloride mixture

In addition to combining multiple nitrate salts, researchers have also explored mixtures of nitrates with chlorides and carbonates. The straightforward preparation of binary eutectic systems has attracted considerable attention due to their potential for lowering melting points and enhancing thermal properties. Zhou et al. [46] synthesized 87% $LiNO_3$-13% NaCl eutectic salts as PCM. The eutectic mixture showed T_m=221.65 ℃ and ΔH=316.5 J/g. They concluded that eutectic PCM were characterized by suitable phase transition temperatures, high fusion

enthalpy, minimal thermal performance degradation after multiple thermal cycles and excellent chemical stability below 400 ℃. Kumar et al. [47] prepared a binary eutectic system of $LiNO_3$ and NaCl, with a T_m=230 ℃ for the mixed salt. In addition to binary mixed salts, ternary mixed salts have also garnered attention. Sang et al. [48] prepared a novel ternary molten salt by adding KCl to a binary nitrate system ($NaNO_3$-KNO_3). They found that the 10% $NaNO_3$-78% KNO_3-12% KCl system exhibited superior phase-change enthalpy and specific heat capacity, demonstrating promising application potential for medium-to-high-temperature thermal energy storage in CSP systems. Li et al. [49] synthesized a novel ternary mixed molten salt $LiNO_3$-KNO_3-KCl. They observed no chemical reactions between the components, demonstrating excellent compatibility. The salt exhibited a low phase transition temperature, high decomposition temperature and outstanding thermal stability during cycling. Furthermore, it showed excellent corrosion resistance against 304 stainless steel, 316 stainless steel and pure aluminum, making it suitable as an encapsulation material. Additionally, Li et al. [50] prepared a ternary molten salt system of 48.08% $LiNO_3$-49.86% $NaNO_3$-2.06% NaCl with high latent heat. This molten salt exhibited a T_m=191.1 ℃, T_d=550 ℃ and ΔH=255.2 J/g. They also found that the mixture had excellent thermal stability during cycling. Castro-Quijada et al. [51] prepared a mixture of solar salt with added NaCl and KCl. The results showed that the T_m ranged from 211 ℃ to 243 ℃, and the T_d ranged from 592 ℃ to 642 ℃. The addition of chlorides improved the thermal stability of the solar salt. The properties of the nitrate-chloride mixtures and their physical information were presented in Table. 6. Furthermore, Lai et al. [52] designed and optimized a novel ternary molten salt mixture of $NaNO_3$-NaCl-NaF. They

demonstrated an 86.7% increase in fusion enthalpy compared to Solar salt, a T_d higher than traditional nitrate molten salts, and thermal storage costs at only 50% of Solar salt and 25% of Hitec salt. This makes nitrate–chloride mixtures promising candidates for efficient thermal energy storage in CSP systems. Notably, these salts can reduce the melting points of pure nitrates by adjusting the mixing ratios, thereby extending their operational temperature range and broadening their potential applications. Compared with pure nitrate systems, mixed nitrate-chloride salts generally have higher melting points, mostly ranging from 200 to 288 ℃. However, their thermal stability is generally improved, with decomposition temperatures ranging from 550 to 650 ℃. The enthalpy of phase transition (ΔH) is significantly increased in some systems, reaching as high as 316.5 J/g. Nitrate-chloride composite salts allow for flexible matching of melting point, enthalpy of phase transition, and thermal stability through component regulation. they will gradually replace some pure nitrate molten salts to meet the TES requirements of different temperature ranges in solar thermal power generation.

Table. 6. Summary of nitrate-chloride hybrid salts.

Component	T_m (℃)	T_d (℃)	ΔH (J/g)	Ref.
87% $LiNO_3$-13% NaCl	221.65	-	316.5	[46]
88.8% $LiNO_3$-11.2% NaCl	230.0	-	302	[47]
10% $NaNO_3$-78% KNO_3-12% KCl	206.12	641.73	110.48	[48]
33.12% $LiNO_3$- 62.64% KNO_3- 4.24% KCl	117.4	553	148.5	[49]
48.08% $LiNO_3$-49.86% $NaNO_3$-2.06% NaCl	191.1	550	255.2	[50]
(25%-60%) $NaNO_3$-(25%-36%) KNO_3-(0-25%)	211-243	592-642	-	[51]

NaCl-(0-25%) KCl				
94% $NaNO_3$-1.8% NaCl-4.2% NaF	288	650	211	[52]

2.4 Nitrate-carbonate mixture

In the nitrate-carbonate system, Na et al. [53] prepared a $NaNO_3$-Na_2CO_3 mixed molten salt. Results indicated the mixed molten salt exhibited a $T_{m,min}$=300.7 ℃, $T_{d,max}$=639 ℃ and a maximum average thermal conductivity of 0.79 W/(m·K). Sang et al. [48] prepared a ternary molten salt mixture of 47% $NaNO_3$-46% KNO_3-7% K_2CO_3. They revealed that the T_d increased to over 640 ℃, significantly higher than conventional solar salts (600 ℃). Moreover, Na et al. [54] experimentally investigated the effect of Na_2CO_3 addition on the thermophysical properties of KNO_3-$NaNO_2$ binary molten salts. Results indicated that adding 7% Na_2CO_3 to the binary molten salt reduced T_m by 5.8%. The addition of 9% Na_2CO_3 increased the T_d by 20.6%, specific heat capacity by 4.8% and thermal conductivity by 7.5%. Sang et al. [55] investigated the thermophysical properties of the ternary eutectic salt 25.9% KNO_3-68.7% KNO_2-5.4% K_2CO_3 through experiments combined with theoretical calculations. The results demonstrated that the eutectic salt had T_m=342.1 ℃ and T_d=750.1 ℃. The thermal properties remained stable after 100 thermal cycles within the temperature range of 30-800 ℃. It effectively met the high-temperature thermal storage material requirements of supercritical CO_2 for CSP systems. The nitrate-carbonate molten salt had a high T_d, as presented in Table. 7. To address issues of low upper operating temperature limits in traditional solar salts, Huang et al. [56] designed and developed a novel quaternary mixed molten salt composed of $NaNO_3$-KNO_3-Na_2CO_3-NaCl. They revealed that this mixture achieved a 21.5 ℃ reduction in T_m and a 55.0 ℃ increase in T_d

compared to solar salts, making it an excellent candidate material for high-temperature thermal storage and heat transfer media in CSP systems. Compared with pure nitrate and nitrate-chloride systems, nitrate-carbonate mixed salts exhibit significantly improved thermal stability, with decomposition temperatures generally exceeding 600 ℃ and reaching as high as 750 ℃. However, their melting points are generally higher, mostly ranging from 200 to 300°C and ΔH is relatively low at 72-114 J/g. The introduction of components such as KNO_3 and $NaNO_2$ can effectively lower the melting point, while increasing the proportion of carbonates can raise the decomposition temperature. However, it is essential to address the issues of high-temperature corrosion and viscosity associated with carbonates. Integrating corrosion-resistant alloys with heat exchanger design will facilitate their engineering application in next-generation solar thermal power plants.

Table. 7. Summary of nitrate-carbonate hybrid salts.

Component	T_m (℃)	T_d (℃)	ΔH (J/g)	Ref.
90% $NaNO_3$-10% Na_2CO_3	298.9	600	-	[53]
80% $NaNO_3$-20% Na_2CO_3	300.1	622	-	[53]
70% $NaNO_3$-30% Na_2CO_3	299.1	639	-	[53]
47% $NaNO_3$-46% KNO_3-7% K_2CO_3.	207.24	642.66	87.12	[48]
51.15% KNO_3-41.85% $NaNO_2$-7% Na_2CO_3	133.1	650.3	72.21	[54]
50.05% KNO_3-40.95% $NaNO_2$-9% Na_2CO_3	140.9	659.9	-	[54]
25.9% KNO_3-68.7% KNO_2-5.4% K_2CO_3	342.1	750.1	114.5	[55]
54% $NaNO_3$-36% KNO_3-6% Na_2CO_3-4% NaCl	199.1	620	111.9	[56]

2.5 Nitrate/nitrate-based corrosion

Pure nitrate PCM inherently possesses some oxidizing properties. Corrosion of common energy storage materials such as carbon steel, stainless steel, and alloy steel is primarily electrochemical in nature [57]. However, the introduction of chloride and nitrite impurity ions into the system can completely alter the corrosion mechanism, significantly exacerbate localized corrosion, and even pose a risk of equipment failure. The corrosion reactions of nitrate and nitrate-based salts are as follows [58, 59].

$$NO_3^- + 2e^- \leftrightarrow NO_2^- + O^{2-} \quad (1)$$

$$Fe + O^{2-} \leftrightarrow FeO + 2e^- \quad (2)$$

$$3FeO + O^{2-} \leftrightarrow Fe_3O_4 + 2e^- \quad (3)$$

$$NO_3^- + O^{2-} \leftrightarrow NO_2^- + O_2^{2-} \quad (4)$$

$$Fe + 2Cr + 4O^{2-} \rightarrow FeCr_2O_4 \quad (5)$$

In stainless steels and nickel-based alloys containing chromium and nickel, a dense spinel-type oxide layer ($FeCr_2O_4$) forms spontaneously on the surface, temporarily preventing molten salt and mitigating uniform corrosion. Cl^- can penetrate or destroy the originally dense oxide protective layer on the metal surface, such as Fe_3O_4 and Cr_2O_3, inducing localized corrosion. NO_2^- exhibits strong oxidizing properties at high temperatures and readily reacts with Cr and Fe in the alloy to form porous layers of oxides or nitrides. When nitrites and nitrates coexist, their redox cycle may continuously deplete the alloy's passivation elements.

The primary factors influencing corrosion behavior include the composition of the molten salt, operating temperature and the composition of the structural materials. Lague et al. [60]

systematically summarized the corrosion mechanisms and challenges associated with nitrates in CSP systems and identified directions for both short-term and long-term research. Based on engineering applications, feasible and effective mitigation strategies should be developed to address the corrosion challenges posed by nitrate-based PCMs containing chloride ions and nitrite ions. These strategies address four key areas: material selection, molten salt modification, surface protection and operating condition control.

2.6 Preparation of mixed salts

The preparation method for mixed molten salts includes three steps: drying treatment, weighing and mixing, and melting followed by cooling treatment, as illustrated in Fig. 3. This methodology has been widely adopted by researchers both domestically and internationally [61-63]. The specific preparation process is as follows: (1) Drying treatment: The single-component salt is placed in an electric hot-air drying box (180 ℃, 48 h) to remove moisture. (2) Weighing and mixing: A high-precision balance is used to weigh single-component salts, which are then thoroughly ground using a mortar and placed in a crucible. (3) Melting and cooling: The sample is placed in a muffle furnace (300 ℃, 12 h) and the mixed salt is prepared using the static melting method. After the sample has completely melted and mixed evenly, the mixed sample is poured into a steel tray to cool naturally. Once crystallized, it is crushed using a crusher and stored in a drying oven.

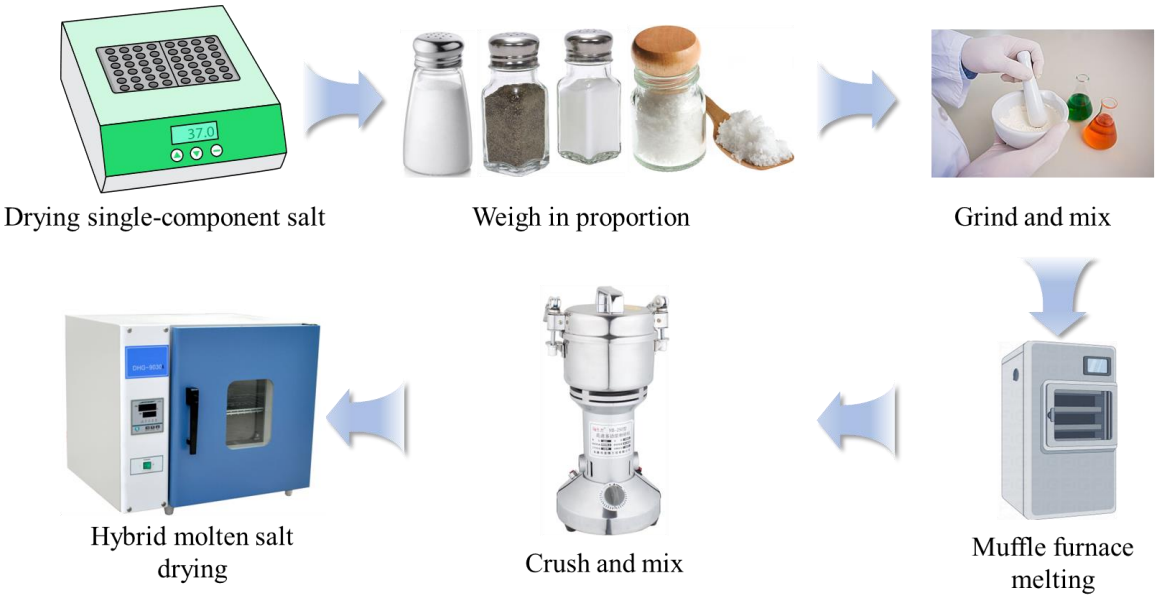

Fig. 3. Preparation method of mixed molten salt.

2.7 Summary

The aforementioned studies revealed that nitrates exhibited a relatively high T_m, typically exceeding 200 ℃ and a low T_d, generally below 600 ℃. Mixing nitrates or adding additional salts to nitrate could modify the melting point of molten salts and optimize their thermal stability to some extent. Molten salts with various temperature ranges and performance characteristics can be developed by appropriately adjusting material ratios to meet the demands of different application fields. In solar thermal power generation systems, low-melting-point molten salts can efficiently store and transfer thermal energy at lower operating temperatures, reducing energy losses and enhancing overall system efficiency. Key thermophysical properties, including melting point, decomposition temperature, thermal conductivity, and heat storage capacity, can be further optimized through rational compositional design, facilitating the development of high-performance molten salt systems for efficient solar energy storage. Consequently, further investigation into the thermal properties and operational performance of

nitrate-based molten salts is essential to advance their application in solar thermal power systems.

3 Performance enhancement of nitrates

As an important heat storage and transfer medium, nitrates exhibit poor thermal conductivity (λ). Therefore, improving thermal conductivity can effectively boost heat charging and discharging capacity [64]. Preparing composite PCM by incorporating high-thermal-conductivity materials, such as carbon-based materials [65], nano-additives [66] and micro-encapsulation technology [67], can significantly improve their thermal conductivity. The method and material for improving thermal conductivity is illustrated in Fig. 4. Three methods for enhancing thermal conductivity are discussed in detail below.

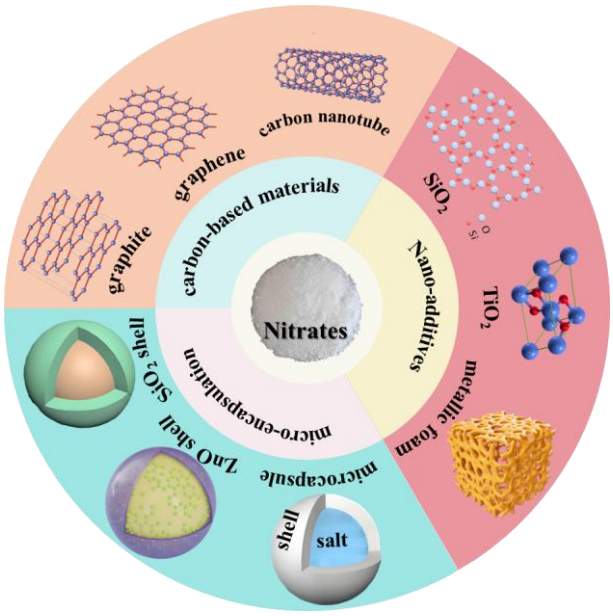

Fig. 4. Approaches to enhancing the thermal performance of nitrates.

3.1 Carbon-based materials

Carbon-based materials possess high structural stability, excellent thermal conductivity

and chemical inertness, making them ideal for providing mechanical support and efficient thermal conduction pathways in phase change materials (PCMs). Common carbon-based materials include carbon nanotubes (CNTs), graphite, and expanded graphene (EG). Carbon nanotubes exhibit exceptionally high thermal conductivity, ranging from 1100 to 7000 W/(m·K), which has motivated extensive research into incorporating CNTs into molten salts to fabricate high-performance composite PCMs. Yu et al. [68] experimentally prepared composite PCM using KNO_3 as the matrix and single-walled carbon nanotubes (SWCNTs) as reinforcements, is presented in Fig. 5(a). Their research revealed that carbon nanotubes could enhance both thermal conductivity and specific heat capacity, but resulted in a decrease in ΔH. Wu et al. [69] prepared composite solar salt materials with varying doping levels of multi-walled carbon nanotubes (MWCNTs) at ratios ranging from 0 to 0.5%, identifying 0.3% as the optimal doping ratio.

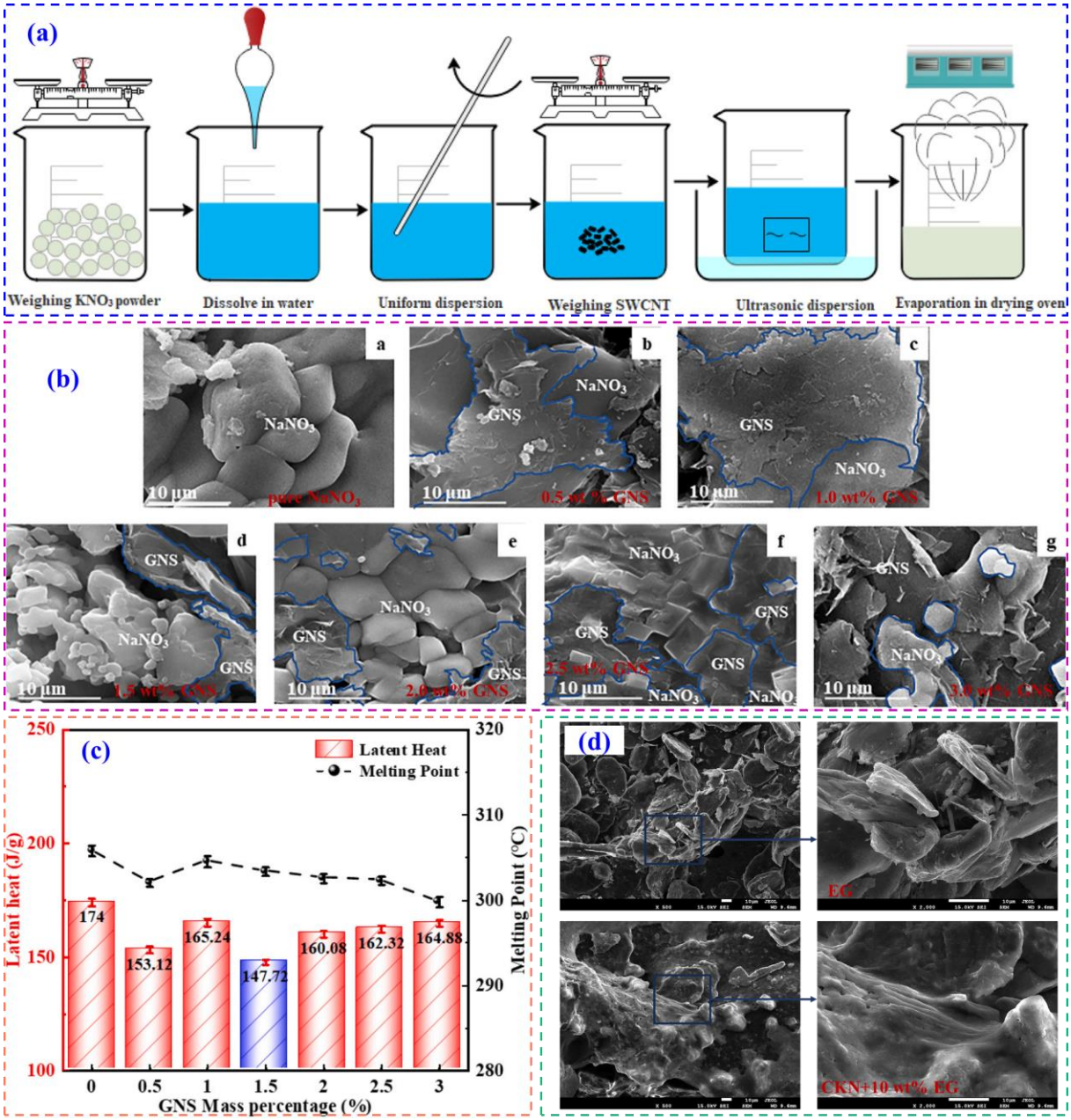

Fig. 5. Approach for enhancing nitrate salts using carbon-based materials, (a) preparation process of PCM with SWCNTs [68], (b) scanning electron micrograph of GNS@$NaNO_3$ [70], (c) melting point and phase change enthalpy[70], (d) SEM images of EG and CMS [71].

Graphene possesses low density, high porosity, superior thermal conductivity and excellent chemical stability, making it suitable for enhancing the thermal conductivity and mechanical properties of molten salts. Lyu et al. [70] proposed a composite phase-change

material with $NaNO_3$ as the matrix and graphene nanosheets (GNS) as the reinforcing agent. The morphology scanning is shown in Fig. 5(b). They found that the thermal conductivity of the composite PCM increased continuously with rising GNS content, reaching a 245% increase at 3.0 wt% doping ratio. Although GNS enhanced thermal conductivity, it reduced T_m and ΔH, as illustrated in Fig. 5(c). Therefore, an optimal doping ratio should be selected to balance thermal conductivity enhancement with ΔH preservation. Zhu et al. [72] summarized recent research advances in enhancing the thermal conductivity of PCMs using graphene-based materials, including graphene, graphene oxide (GO), functionalized graphene/GO and graphene aerogel (GA). They analyzed their applications in solar energy and battery thermal management.

EG has become a research focus due to the low cost, the high thermal conductivity, excellent adsorption properties, and the strong chemical stability [73]. Li et al. [74] prepared $LiNO_3$-NaCl/EG composite PCM with EG mass fractions of 10%, 15%, 20%, and 30%. Experimental results indicated that as the mass fraction of EG increased, the T_m and ΔH of the composite PCM gradually decreased, while the thermal conductivity increased. In related work, Li et al. [75] prepared a $NaNO_3$-$LiNO_3$-NaCl/EG composite material. When the EG content was 20%, the molten salt exhibited a thermal conductivity of 5.017 W/(m·K). Li et al. [76] investigated the effect of EG on $LiNO_3$-$NaNO_3$-KCl mixed molten salts, finding that EG could enhance thermal conductivity and reduce supercooling. They reported that a 15%–20% EG content could balance thermal storage capacity and heat transfer efficiency. Wu et al. [71] investigated the enhancement mechanism of EG on the thermal conductivity of KNO_3-$NaNO_2$-(Ca $(NO_3)_2 \cdot 4H_2O$ (CKN) ternary nitrate, as illustrated in Fig. 5(d). Their study revealed that the

thermal conductivity surged after EG incorporation, reaching 8.171 W/(m·K) at 20 wt% EG. However, after EG exceeded 20%, the thermal conductivity decreased due to the aggregation of EG particles, which disrupted the heat transfer pathways. The addition of carbon-based materials such as EG and other materials to pure molten salts enhances thermal conductivity. However, the reduction in molten salt content leads to decreased heat capacity. Furthermore, these materials also lower T_d and ΔH. Therefore, appropriate components should be selected to improve thermal conductivity. It is recommended to develop high-thermal-conductivity composite carbon-based materials, including graphene, carbon nanotubes, and porous carbon. This approach enhances thermal conductivity with minimal additions, mitigating the reduction in thermal capacity caused by a decrease in the molten salt content.

3.2 Nanoparticles additives

Metal oxides have attracted widespread attention for improving the low thermal conductivity of nitrates, owing to their chemical stability and distinctive structural characteristics. Common metal oxides include copper oxide (CuO), titanium oxide (TiO_2), aluminum oxide (Al_2O_3), magnesium oxide (MgO) and iron oxide (Fe_2O_3). Myers et al. [77] modified KNO_3, $NaNO_3$ and KNO_3-$NaNO_3$ mixtures using CuO nanoparticles as a modifier. The study found that CuO enhanced heat transfer performance while maintaining chemical stability. It demonstrated the most pronounced enhancement effect on KNO_3-$NaNO_3$ mixtures, with 2 wt% significantly improving heat transfer performance without compromising thermal storage density. In subsequent research, Son et al. [78] prepared porous CuO nanowires to optimize $LiNO_3$ performance, as illustrated in Fig. 6(a). The incorporation of 7 vol% CuO

443 nanowires enhanced thermal conductivity by 6.7 times and increased charge/discharge rates by
444 1.3 times compared to pure $LiNO_3$, with no significant performance degradation after 100
445 thermal cycles. Awad et al. [79] dispersed CuO, Fe_2O_3 and TiO_2 nanoparticles at concentrations
446 of 0.5-1.5 wt% into solar salts. They found that Fe_2O_3 was the most effective in improving λ
447 and specific heat (c_p). The λ increased by 45.01% compared to pure salt at 0.5 wt% and the c_p
448 increased by 10.5% compared to pure salt at 1.5 wt%. Meanwhile, CuO demonstrated the most
449 pronounced effect on ΔH, increasing it by 14.45% at 1 wt% relative to pure salt. Hu et al. [80]
450 employed freeze-drying method to prepare solar salts modified with Al_2O_3 nanoparticles, as
451 illustrated in Fig. 6(b). They found that Al_2O_3 particles effectively optimized the thermal
452 properties of solar salts within the 0-2.0 wt% range, with c_p monotonically increasing with
453 Al_2O_3 content. Wei et al. [81] prepared solar salts modified with 2.5 wt%-10.0 wt% MgO
454 nanoparticles. The properties of solar salts first improved and then stabilized with increasing
455 MgO content. The 5wt% MgO solar salts demonstrated optimal performance and held great
456 promise for application in high-temperature thermal storage and heat transfer within CSP
457 systems. The SEM image shown in Fig. 6(c).

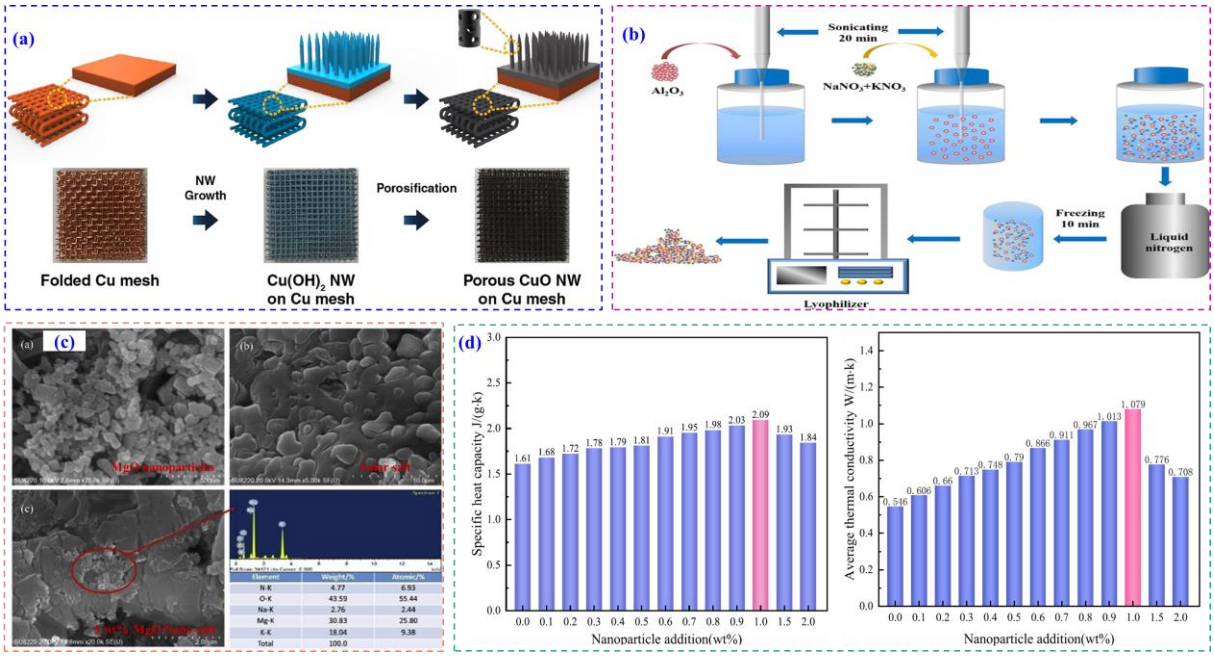

458

459 **Fig. 6.** Approach for enhancing nitrate salts using nanoparticles, (a) synthesis of porous CuO

460 [78], (b) preparation PCM with nanoparticles using freeze-drying method [80], (c) SEM image

461 for MgO and MgO solar salt [81], (d) c_p and λ of TNC-MS with SiO_2 [82].

462 In addition to incorporating metal oxides, studies have shown that the addition of SiO_2 can

463 further enhance the thermophysical properties of molten salts. Jeong et al. [83] conducted

464 research on the enhancement of c_p of KNO_3 by SiO_2 nanoparticles and found that there was an

465 optimal SiO_2 concentration of 1 wt%, with a maximum increase of 24.1%/28.1% in solid/liquid

466 state. However, concentrations exceeding 1 wt% caused particle agglomeration, resulting in

467 decreased c_p. El Far et al. [84] synthesized molten salt nanofluids by dispersing SiO_2

468 nanoparticles in a binary $NaNO_3$-KNO_3 mixture. Results showed that 1 wt% SiO_2 nanoparticle

469 increased the c_p by 15%. In related work, Meng et al. [82] investigated the effects of adding

470 SiO_2 nanoparticles at different mass fractions to a ternary nitrate-carbonate molten salt (TNC-

471 MS) on thermophysical properties. SiO_2 nanoparticles exerted no significant influence on the

472 thermal stability of the molten salt, with T_m=140.2 ℃ and T_d=688 ℃. Moreover, the c_p and λ

first increased and then decreased with SiO_2 content. The average c_p and λ containing 1 wt% SiO_2 were 29.6% and 97.9% higher than those of the base salt, respectively, as shown in Fig. 6(d).

The combined effect of incorporating two different types of nanoparticles on the thermophysical properties of molten salts has received relatively limited attention. Tian et al. [85] prepared SiO_2/MgO composite nanoparticles to modify Hitec salt. It was demonstrated that the addition of nanoparticles slightly reduced the T_d. The combination of 0.3% SiO_2+0.7% MgO yielded the optimal results, with an average c_p increase of 54.3% and λ improvement of 13.13%. Xiao et al. [86] proposed a composite modification strategy using Al_2O_3 nanoparticles and metal foams (copper/nickel) to enhance the low λ of solar salts. Their study showed that copper foam/2 wt% Al_2O_3 reduced charging time by 74% at 240 ℃, significantly improving the thermal response speed of latent heat thermal energy storage (LHTES) units. Wong et al. [87] prepared MWCNT/TiO_2 composite nanoparticles and doped them into quinary nitrate. Experimental studies revealed a 94.77% reduction in viscosity, 17.66% increase in c_p, 37.78% increase in ΔH and a 25.41% increase in λ when using 0.05 wt% MWCNT and 0.01 wt% TiO_2 nanoparticles. Yu et al. [88] investigated the addition of SiO_2/TiO_2 nanoparticles at different ratios to improve the c_p and λ of quaternary nitrate molten salts. When 0.1 wt% SiO_2 and 0.9 wt% TiO_2 was added, the c_p increased by 28.1% and λ rose by 53.7% compared to the pure quaternary salt. Research conducted both domestically and internationally has demonstrated that modifying nitrates by preparing molten salt nanofluids through the addition of nanoparticles can significantly enhance the thermal conductivity λ of PCMs. This strategy also

494 improves the specific heat capacity c_p and overall heat transfer performance of molten salts,
495 offering new opportunities for their application in thermal energy storage and heat transfer
496 systems.

497 **3.3 Encapsulation technology**

498 A significant challenge in CSP systems is the corrosion of equipment caused by molten
499 salts. To mitigate this issue, microencapsulation technology has emerged as a promising
500 solution. By encapsulating PCMs within a protective shell, this approach prevents direct contact
501 between molten salts and equipment, thereby effectively reducing corrosion and enhancing
502 system longevity. It not only increases the heat transfer area but also enhances the stability of
503 PCMs. Our previous work [89] summarized methods for preparing microencapsulation,
504 including physical , chemical and physical-chemical methods. Albdour et al. [90] not only
505 summarized encapsulation methods but also compared encapsulation approaches at various
506 scales, including macro, micro, and nano-scale encapsulation. Chen et al. [91] prepared
507 SiO_2@$NaNO_3$ core-shell microcapsules, utilizing the SiO_2 shell to address leakage and
508 corrosion issues while enhancing thermal conductivity. Moreover, Lee et al. [92] proposed a
509 water-in-oil (W/O) emulsion-sol-gel method for preparing SiO_2-coated solar salt nanocapsules,
510 as shown in Fig. 7(a). They found that the SiO_2 shell significantly enhances thermal stability,
511 making it suitable for high-temperature thermal storage applications in CSP systems.

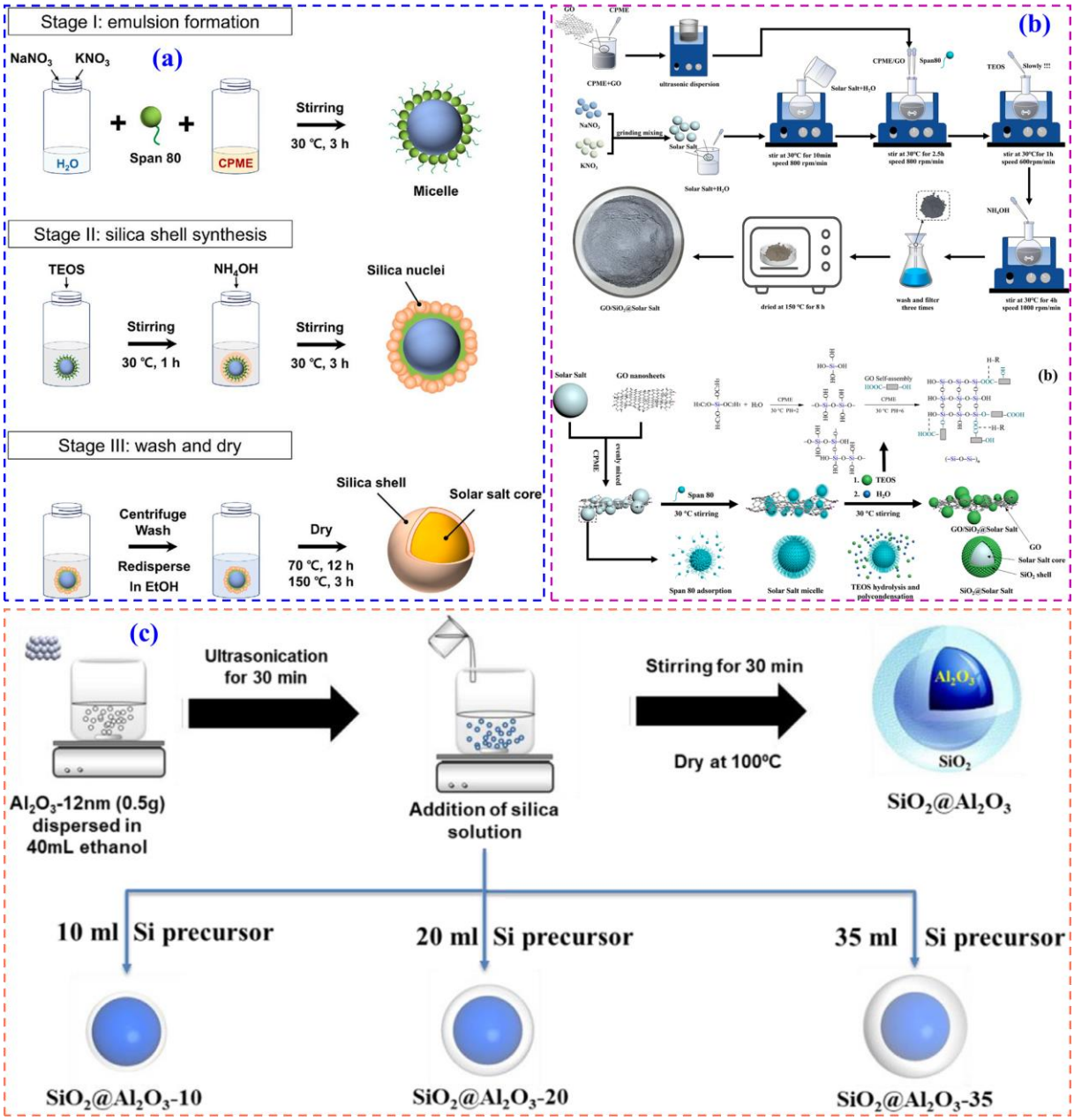

Fig. 7. Microencapsulation method for nitrates, (a) three-step microencapsulation of SiO_2 solar salts [92], (b) microcapsulation process GO/SiO_2@Solar Salt [93], (c) synthesis of SiO_2/Al_2O_3@binary nitrate salt [94].

Besides the aforementioned research on single-shell encapsulation, studies on multi-shell encapsulation have also been explored. Ji et al. [93] encapsulated Solar Salt by combining GO with SiO_2, as illustrated in Fig. 7(b), which significantly enhanced thermal properties, solar-to-

thermal conversion efficiency and cycle stability. Nithiyanantham et al. [94] proposed SiO_2/Al_2O_3 core-shell nanoparticles to enhance the stability and thermophysical properties of nitrates, as displayed in Fig. 7(c). The study revealed that SiO_2/Al_2O_3-35 core-shell particles form chain-like interconnected structures, providing continuous pathways for heat transfer and increasing λ by up to 19%.

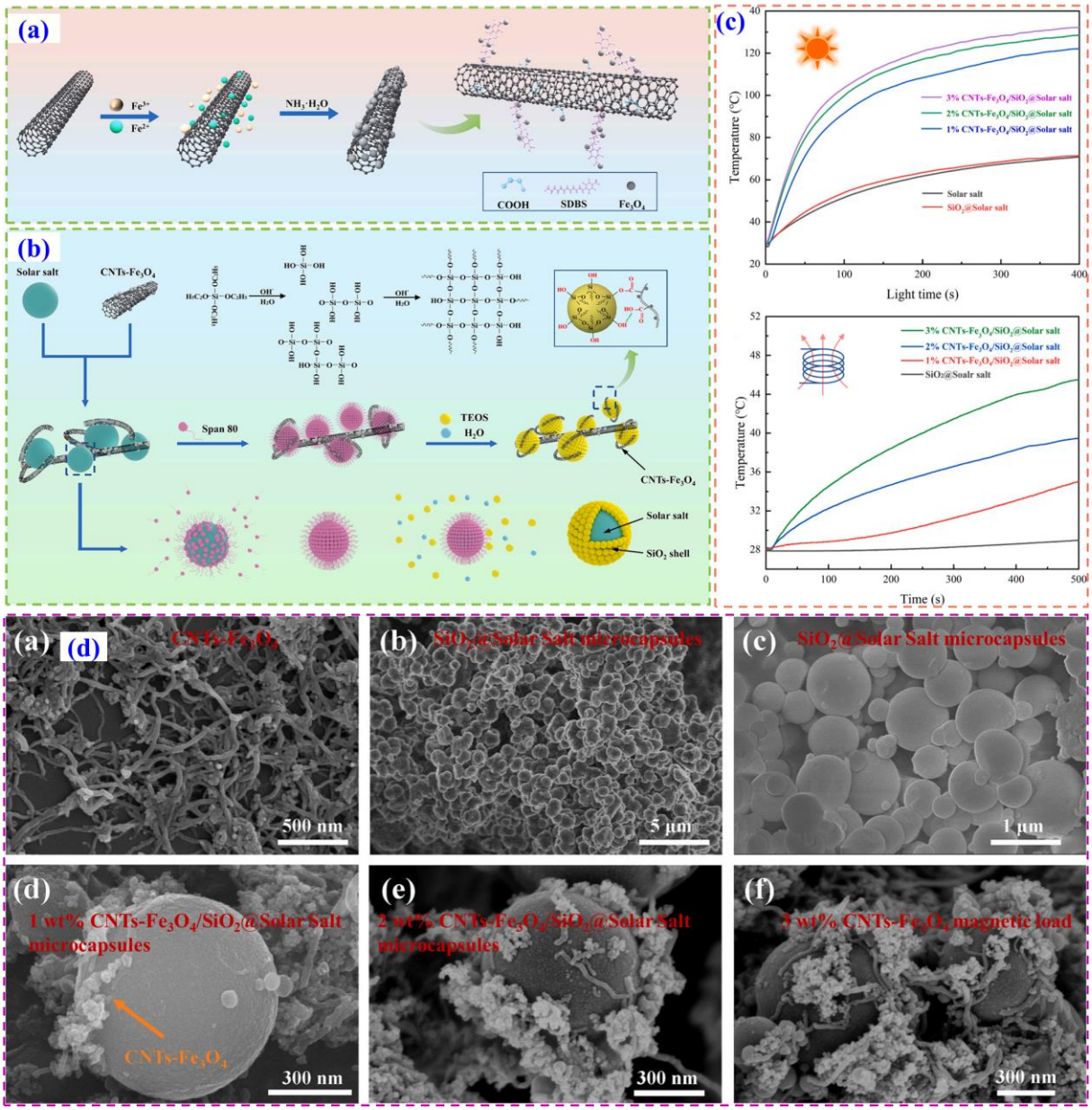

Fig. 8. Microencapsulation of CNTs-Fe_3O_4/SiO_2@Solar salt, (a) magnetic load materials [95], (b) synthetic principle[95], (c) photothermal and magnetic to thermal conversion [95], (d) SEM

micrograph [95].

Wang et al. [95] developed a CNTs-Fe_3O_4/SiO_2@Solar Salt magnetic phase-change microcapsule by encapsulating a molten salt core within a SiO_2 shell and combining it with Fe_3O_4-functionalized carbon nanotubes (CNTs-Fe_3O_4). The study revealed that CNTs-Fe_3O_4 enhanced λ by up to 53.4%, increased T_d by 32 ℃ and exhibited no leakage and shape stability at high temperatures, meeting the long-term TES requirements for CSP. They observed that SiO_2 has negligible effect on photothermal conversion, while the light absorption and conversion properties of carbon nanotubes, combined with the full-spectrum absorption capabilities of Fe_3O_4 nanoparticles, can significantly enhance the absorption performance and photothermal conversion efficiency of PCMs. The synthesis process, performance and SEM images of CNTs-Fe_3O_4 is shown in Fig. 8 [95]. Recently, Xiao et al. [96] focused on the leakage and equipment corrosion issues associated with high-temperature molten salts used in CSP. They summarized three encapsulation methods, melt infiltration, capsule encapsulation and mixed sintering. They pointed out that the multi-shell structure addresses high-temperature stability issues and is suitable for ultra-high-temperature, packed-bed thermal storage, but microcapsule preparation is complex and costly. Ren et al. [97] summarized current methods for improving the thermal conductivity of nitrates and compared the corrosion characteristics and economic costs of solar salt and Hitec salt in CSP systems.

3.4 Summary

Carbon-based materials, nanoparticles, and microencapsulation technologies represent the main strategies for enhancing the performance of nitrate salt PCMs. Carbon-based materials,

548 such as graphene and carbon nanotubes, with thermal conductivities typically exceeding
549 500 W/(m·K), can improve the thermal performance of molten salts by 30%–80%. They also
550 inhibit oxidation and decomposition at high temperatures, while their porous structures can
551 adsorb molten salts to prevent leakage. However, their complex manufacturing processes may
552 introduce impurities, and the high cost of materials, especially graphene, limits large-scale
553 applications. Nanoparticles can enhance the specific heat capacity and convective heat transfer
554 of molten salts, delay solidification and crystallization, and broaden the phase transition
555 temperature range. Nevertheless, challenges remain in their preparation and dispersion, as
556 nanoparticles are prone to agglomeration and sedimentation, which can degrade performance.
557 Microencapsulation effectively prevents leakage, maintains stable phase-change volumes and
558 mitigates corrosion. Yet, its disadvantages include complex fabrication, high cost and reduced
559 overall thermal storage capacity due to the encapsulating shell. While all three technical
560 approaches improve the thermal conductivity of nitrate-based PCMs, they exhibit significant
561 differences in terms of cost, fabrication complexity and scalability. Carbon-based materials,
562 particularly EG, offer the best overall performance. Nanoparticle additives deliver high
563 performance but are costly and difficult to disperse, while encapsulation techniques prioritize
564 structural stability but offer limited thermal conductivity gains and are the most expensive. A
565 comparison of the three methods is presented in Table. 8. Clearly, each method has its own
566 advantages and limitations. EG composites, which balance cost and scalability, are suitable for
567 large-scale solar thermal power generation applications. It is recommended to adopt a
568 composite approach combining a carbon-based scaffold (EG) with low-dose nanoparticles

569 (Al_2O_3/SiO_2) to achieve multiple objectives, including enhanced thermal conductivity,
570 structural stability, cost control, and scalability.

571 **Table. 8.** Comparison of reinforcement methods.

Methods	Carbon-based material	Nanoparticles additives	Encapsulation technology
Cost	Low	Medium to high	High
fabrication complexity	Medium to high	High	High
Scalability	Medium	Low	Medium to high
Advantages	Significant improvement in thermal conductivity	Improves specific heat capacity and aids heat transfer	Prevents leakage and ensures structural stability
Limitations	High addition levels may reduce latent heat	Agglomeration and failure after long-term cycling	High cost and complex preparation

572 **4 Casing heat accumulator**

573 With the development of new energy systems and the rapid expansion of the energy storage
574 market, phase change heat accumulators have become a key technology for solving the problem
575 of energy supply and demand matching due to their high heat storage density. Phase change
576 heat accumulators can be classified into casing type, shell-and-tube type, plate type and spiral

tube type based on their structural design, as shown in Fig. 9. Among these, casing and shell-and-tube heat storage devices have become research hotspots due to their simple structure and high heat transfer efficiency. The thermal storage efficiency of accumulators can be improved by increasing the thermal conductivity of the PCM mentioned in Section 3 and expanding the heat transfer surface area of the thermal storage structure. This can be achieved through pipe optimization, fin addition, topological optimization and biomimetic optimization [98]. Subsequent sections will discuss these various methods in detail.

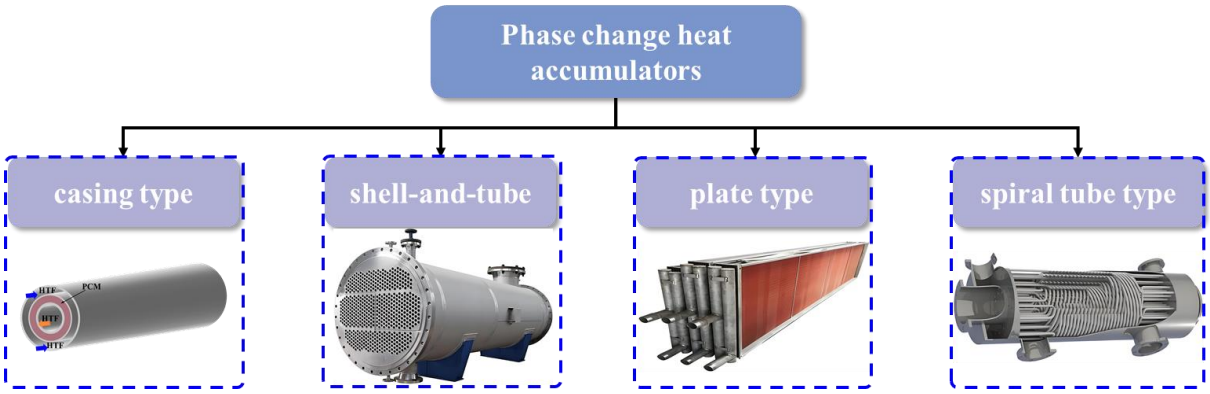

Fig. 9. Classification of phase change heat accumulator.

4.1 Tube construction

The positioning and geometry of pipes within phase change heat accumulators are critical factors that significantly influence their thermal storage and release performance. Mao et al. [99] proposed an eccentrically helical shell-and-tube heat storage tank. Results indicated that the optimal eccentricity can reduce melting time by 47.19% and increase the average heat storage rate by 83.85% compared to non-eccentric configurations. The liquid fraction distribution for different eccentricities is shown in Fig. 10(a). Zheng et al. [100] designed bidirectionally twisted tubes and investigated the influence of their structural parameters on

molten salt heat transfer performance. It was found that twisted tubes can significantly enhance the heat transfer of molten salt nanofluids, with *Nu* increasing by up to 20% compared to smooth tubes. Bidirectionally twisted tubes further optimized heat transfer through counter-twisting, with the optimal performance *PEC*=1.13 achieved at *n*=2 counter-twist cycles. Ye et al. [101] conducted numerical studies on L-shaped heat storage units, as shown in Fig. 10(b). Compared with traditional horizontal and vertical units of the same volume, the L-shaped unit exhibited the fastest melting rate during the initial melting phase. Moreover, increasing the radial eccentricity of the inner tube significantly shortened the total melting time. Li et al. [102] investigated the effects of twisted elliptical inner tube structure and annular fin distribution on the PCM melting process, as shown in Fig. 10(c). They found that the twisted elliptical tube enhanced fluid mixing between the core and wall by inducing spiral flow in the HTF, thereby increasing the average wall temperature. The annular fins significantly accelerated PCM melting by expanding the heat transfer area and intensifying local natural convection. In related study, Eisapour et al. [103] designed a novel elliptical double-tube heat accumulator, as illustrated in Fig. 10(d). The elliptical tubes incorporated corrugated, twisted, and corrugated-twisted configurations featuring distinct wave characteristics and pitch lengths. The study concluded that the descending wave amplitude of the corrugated-twisted configuration represented the most effective waveform. Moghadam et al. [104] investigated the thermal performance of three distinct shell geometries under varying flow conditions. Results indicated that the trapezoidal shell exhibited the highest melting efficiency, while the spherical shell demonstrated the highest solidification efficiency. Khedher et al. [105] conducted a numerical

study on the effect of embedding a framework structure on the inner surface of a heat storage outer tube on melting performance. The results indicated that the framework structure significantly enhanced heat transfer by increasing the contact area between the heat transfer fluid (HTF) and PCM. The melting time for the framework structure was reduced by 55% compared to the structure without a framework.

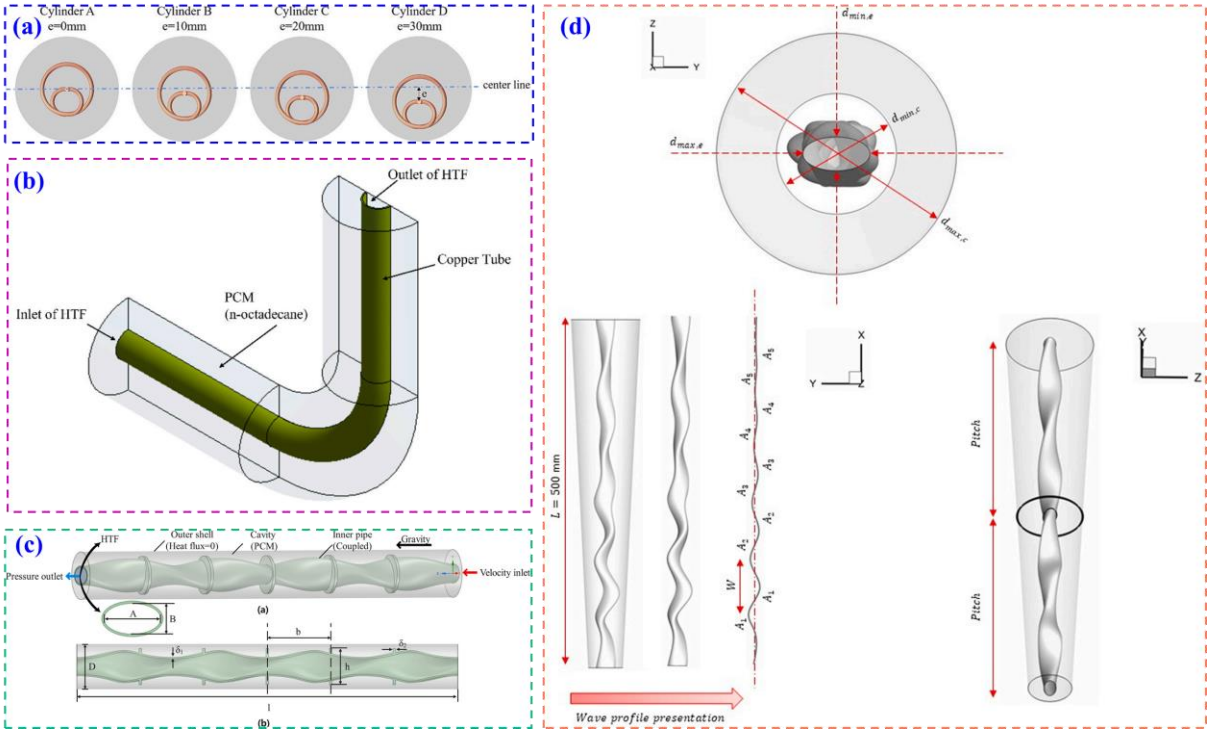

Fig. 10. Diagram of pipeline structure modification, (a) eccentric pipe [99], (b) half of the physical model of L-shape pipe [101], (c) twisted elliptical inner tube structure and annular fin [102], (d) twisted shape pipe [103].

4.2 Extend surface using fins

Fins effectively promote heat exchange within PCMs, accelerating the melting and solidification processes. Extending the surface area with fins significantly enhances the heat transfer efficiency of PCMs by increasing the exposure area. In thermal storage equipment, the

628 rational arrangement and optimized design of fins can effectively enhance the heat transfer
629 efficiency of phase change heat accumulators, thereby achieving high-efficiency thermal
630 storage.

631 Deng et al. [106] investigated the melting performance of PCM under four longitudinal fin
632 arrangements, as illustrated in Fig. 11(a). Results showed that straight fins enhanced top and
633 bottom heat conduction while strengthening lateral natural convection. Inclined fins suppressed
634 the effect of natural convection on the bottom PCM. Bottom fins enhanced lower heat transfer,
635 promoting uniform melting, conversely, top fins increased upper heat transfer, leading to non-
636 uniform PCM melting. Yang et al. [107] designed annular fins to enhance PCM melting, as
637 shown in Fig. 11(b). Numerical simulations investigated the influence of annular fin parameters
638 on PCM melting, revealing that LHTES units with annular fins exhibited superior thermal
639 performance, reducing complete melting time by 65%. Wu et al. [108] designed stratified fins
640 to enhance the performance of phase change heat accumulator, as displayed in Fig. 11(c). They
641 found that stratified fin structure effectively eliminated dead zones between tubes and
642 temperature stratification in the upper layer, reducing melting time by 31.6% and temperature
643 homogenization by 30.4%. Mahdi et al. [109] conducted numerical analysis on the melting of
644 PCM in three-tube system under different fin arrangements. Results indicated that more long
645 fins in the lower half reduced melting time compared to a three-tube thermal accumulator with
646 the same PCM volume. Rashid et al. [110] conducted a numerical analysis on the number of
647 fins in a cylindrical shell-and-tube thermal accumulator affecting PCM melting. The study
648 revealed that the number of fins significantly impacts melting, with the maximum reduction in

operating time reaching 81.4%.

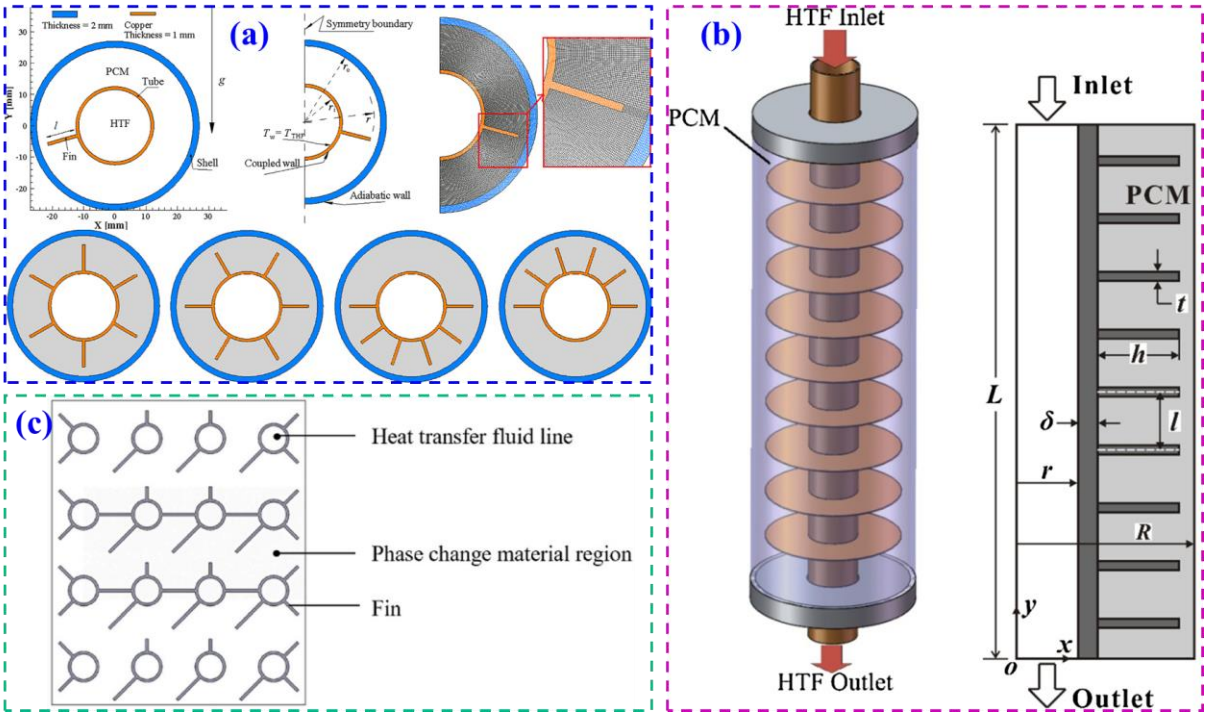

Fig. 11. Layout of different fins, (a) four longitudinal fin arrangements [106], (b) annular fins [107], (c) stratified fin structure [108].

Further studies have shown that optimizing the geometry of fins can lead to more efficient heat transfer. Tavakoli et al. [111] investigated sinusoidal fins inside heat accumulators. Results indicated that the optimal case with sinusoidal internal fins increased liquid fraction by 62% and reduced entropy generation by 59.5% compared to simple straight fins. Agrawal et al. [112] proposed a corrugated annular fin structure, and noticed that it reduced PCM temperature inhomogeneity by 57% through enhancing local turbulence and natural convection. Raj et al. [113] proposed a novel C-shaped fin (see Fig. 12(a)) design that effectively utilized natural convection within the molten PCM. Research demonstrated that C-shaped fins could reduce melting time by up to 59% compared to traditional fin designs. Wang et al. [114] designed a three-tube Y-type finned heat accumulator and found that the Y-type fins delivered optimal

663 performance. The complete melting time was reduced by 31.8%, the average heat absorption
664 rate increased by 48.39%, and temperature uniformity was significantly superior to other
665 designs. Wang et al. [115] conducted a simulation study on the melting/solidification
666 characteristics of PCM in horizontal double-tube heat accumulator with elliptical fins, as
667 illustrated in Fig. 12(b) . The results revealed that incorporating high-aspect-ratio elliptical fins
668 significantly enhanced convective heat transfer at the top and bottom of the annular space,
669 achieving a maximum melting enhancement rate of 16.9% and a solidification enhancement
670 rate of 13.8%. Wołoszyn et al. [116] proposed a novel spiral-wound shell-and-tube heat storage
671 device incorporating helical fins and varying shell-tube geometries. Results demonstrated that
672 compared to vertical and horizontal configurations, the proposed device significantly reduced
673 PCM melting and solidification times. Guo et al. [117] proposed a novel inclined fin with
674 bending angles ranging from 0° to 75° both upward and downward, as illustrated in Fig. 12(c).
675 Results demonstrated that the fin with downward bending angle of 10° shortened the complete
676 heat storage time by 55.41% and improved temperature uniformity by 20.00%. Zhang et al.
677 [118] proposed a heat accumulator with helical fins as shown in Fig. 12(d). Simulation results
678 indicated that shortening the helical pitch and increasing the number of fins can accelerate the
679 melting rate. Moreover, the fully melted state is achieved in the shortest time when the
680 accumulator is placed horizontally, reducing the time by 14.3% compared to vertical placement
681 and preventing uneven melting. In subsequent research, Lv et al. [119] designed four types of
682 heat accumulators with longitudinal, H-shaped, helical, and finless configurations.
683 Experimental results indicated that the helical fins exhibited the best heat transfer performance

during the charging process.

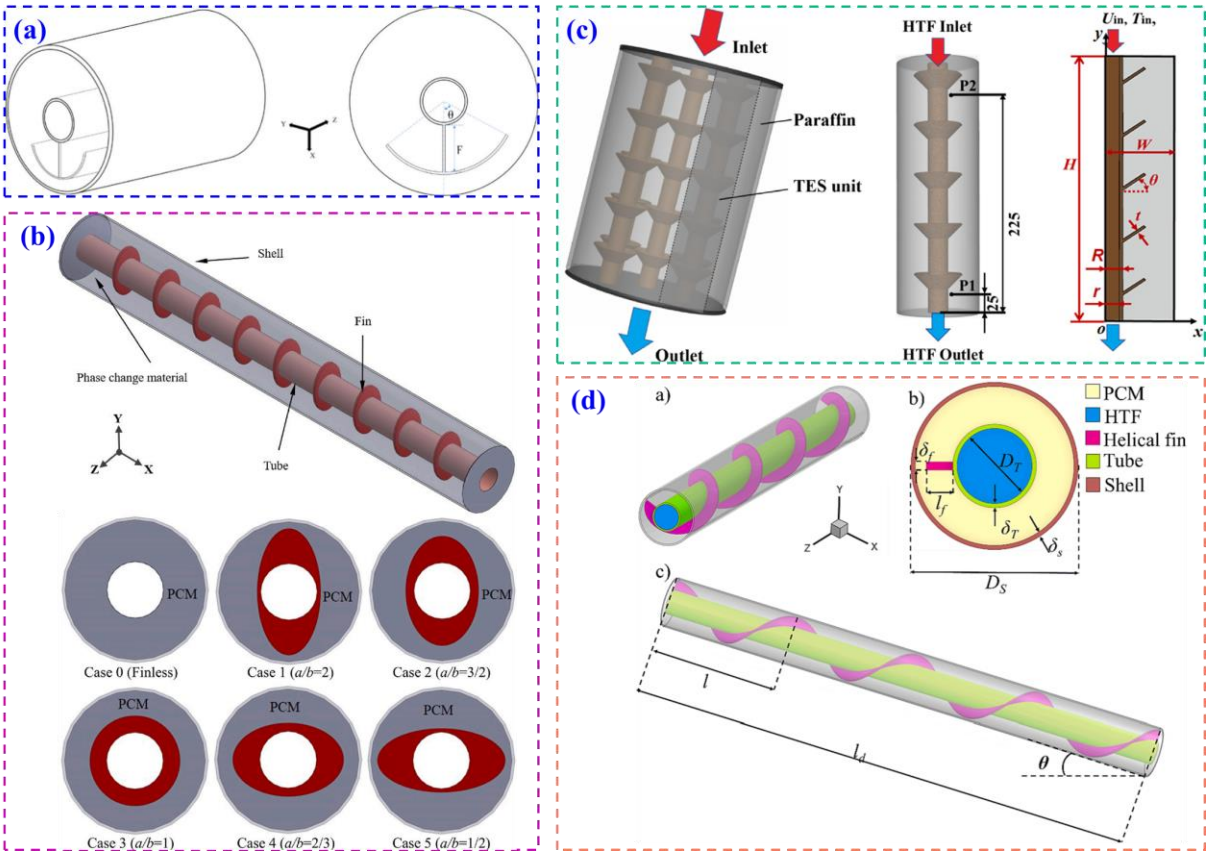

Fig. 12. Fin shape modification structure, (a) C-shaped fins [113], (b) elliptical fins [115], (c) Inclined fins [117], helical fins [118].

Liu et al. [120] designed a composite fin integrating the advantages of longitudinal and annular fins. Results showed that the composite fin reduced melting time by 21.6% and 9.5%, respectively, compared to longitudinal and annular fin models. Tang et al. [121] designed novel discontinuous fins to enhance heat transfer efficiency. Research revealed that discontinuous fins shortened the complete melting time of PCM by 23.4% and improved temperature uniformity by 36.7% compared to traditional longitudinal straight fins. Recently, Izadi et al. [122] summarized the effects of fins on melting and solidification, including the influence of annular fins, longitudinal fins, and fin geometric parameters.

4.3 Topology optimization

Traditional fin designs rely on empirical knowledge and fixed geometries, failing to adequately account for complex heat flux distributions and structural optimization. Consequently, conventional approaches limit heat exchange efficiency, potentially resulting in material wastage and suboptimal utilization. Topology optimization, however, can automatically generate optimal structural shapes tailored to specific heat flux and structural requirements, thereby reducing material waste. Zhang et al. [123] combined topology optimization theory with LTES solid-liquid phase change heat transfer to establish an optimized design method for LTES fins. The topology-optimized fins (see Fig. 13(a)) reduced discharge time by 31% compared to conventional fins, making them more suitable for rapid heat dissipation scenarios. Laasri et al. [124] compared topology optimization design with a single and double tube LHTES device without fins, and found that topology optimization design significantly improved performance, with a maximum performance improvement of 86.3%. Ge et al. [125] investigated the discharge process of a shell-and-tube heat accumulator equipped with topologically optimized fins. The results demonstrated that the topologically optimized device exhibited superior performance, with discharge time reduced by 57.1%. Chen et al. [126] conducted numerical simulations of the phase-change heat transfer process in a heat accumulator by integrating eccentricity optimization and topology optimization techniques. The results demonstrated that the heat storage rate increased by 36.43% and the heat release rate improved by 15.53% compared to the topology-optimized structure without eccentricity. Zhang et al. [127] employed a topology optimization method based on different optimization

objectives to develop a fin structure, as shown in Fig. 13(b). The results demonstrated that the naturally generated topology exhibited excellent thermal conductivity, effectively enhancing heat storage efficiency. He et al. [128] proposed a novel fin structure capable of evolving throughout the optimization process, as displayed in Fig. 13(c). Results demonstrated that the topologically optimized fins more effectively elevated the temperature and liquid fraction of the PCM compared to conventional rectangular fins. The above studies demonstrate that topology optimization, as an efficient design tool, offers significant advantages in enhancing the performance of heat exchanger systems in thermal accumulators. This approach not only addresses the limitations of traditional designs but also offers innovative solutions for the future development of thermal energy storage and conversion technologies.

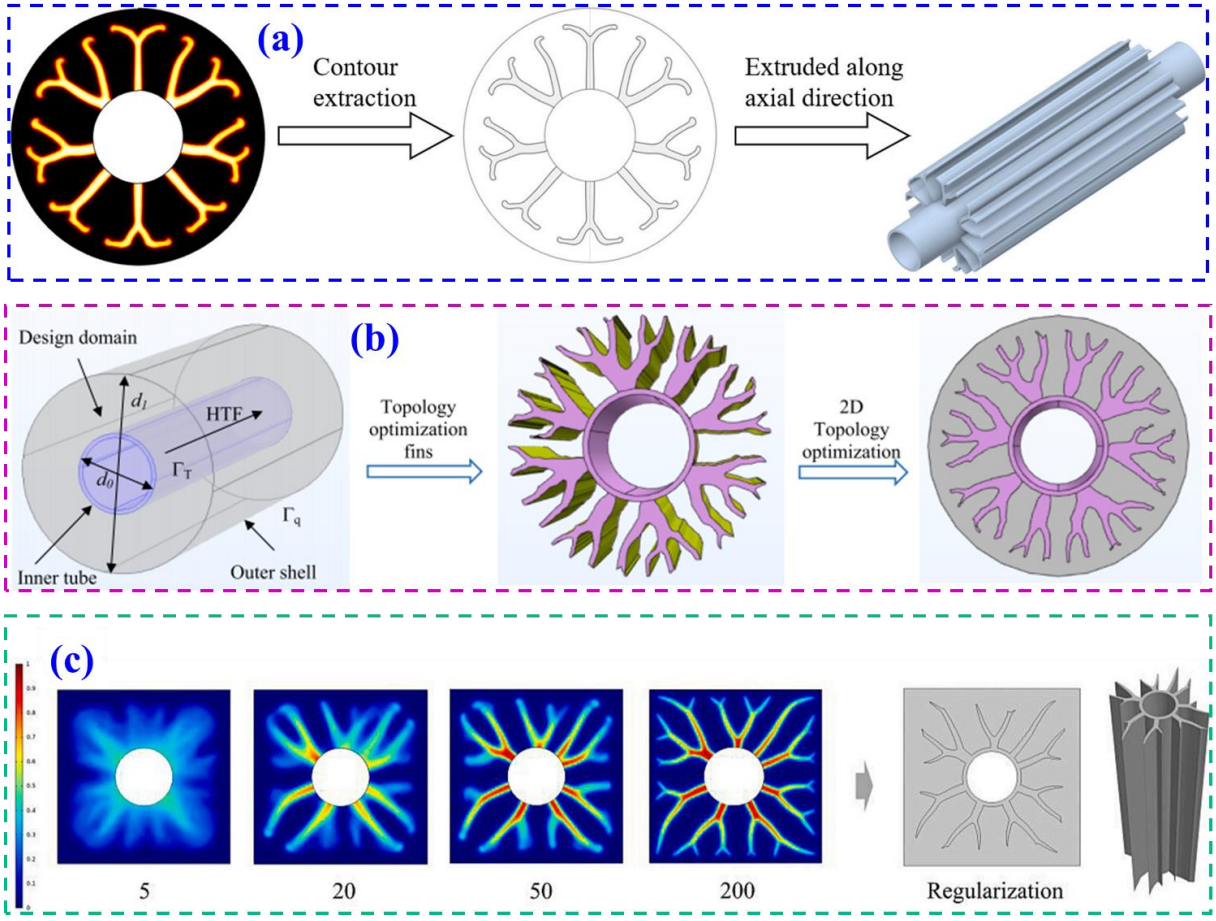

Fig. 13. Topology optimization structure, (a) topology optimized fin structures [123], (b) Topology-optimized geometric model [127], (c) regularization of topology optimized fins [128].

Research on fin topology optimization design has revealed that the incorporation of branching fins significantly enhances heat transfer performance. Song et al. [129] proposed a novel 3D anisotropic fractal fin structure, as shown in Fig. 14(a). They found that the uniformly dispersed fractal fins enhanced heat conduction while reducing resistance to natural convection, achieving synergistic enhancement of heat conduction and convection. Li et al. [130] developed a non-uniform Y-shaped fractal fin, as illustrated in Fig. 14(b). Results demonstrated that the application of fractal fins enhances the performance of thermal storage devices, exhibiting superior heat transfer rates and temperature control capabilities. In subsequent research, Liu et al. [131] designed non-uniformly distributed Y-shaped fins. Comparative studies with uniform fins revealed that the lower Y-shaped fins significantly reduced melting time, shortening the complete melting time by 21.5%. Yan et al. [132] proposed a Y-shaped fin structure on both inner and outer surfaces, as shown in Fig. 14(c). Results indicated that reducing fin thickness and increasing fin angle effectively shortened PCM melting time. Ao et al. [133] investigated the influence of V-shaped fin (see Fig. 14(d)) parameters and arrangement patterns on the heat transfer performance of heat storage units. The optimal fin structure achieved a heat storage efficiency 2.57 times higher than the finless structure, with a 61.05% reduction in charging time. In related study, Yao et al.[134] conducted a numerical study on the heat storage performance of different V-shaped fin arrangements. Results indicated that optimally arranged V-shaped fins reduced the PCM melting time in the heat accumulator by 31.92% compared to conventional

rectangular fins.

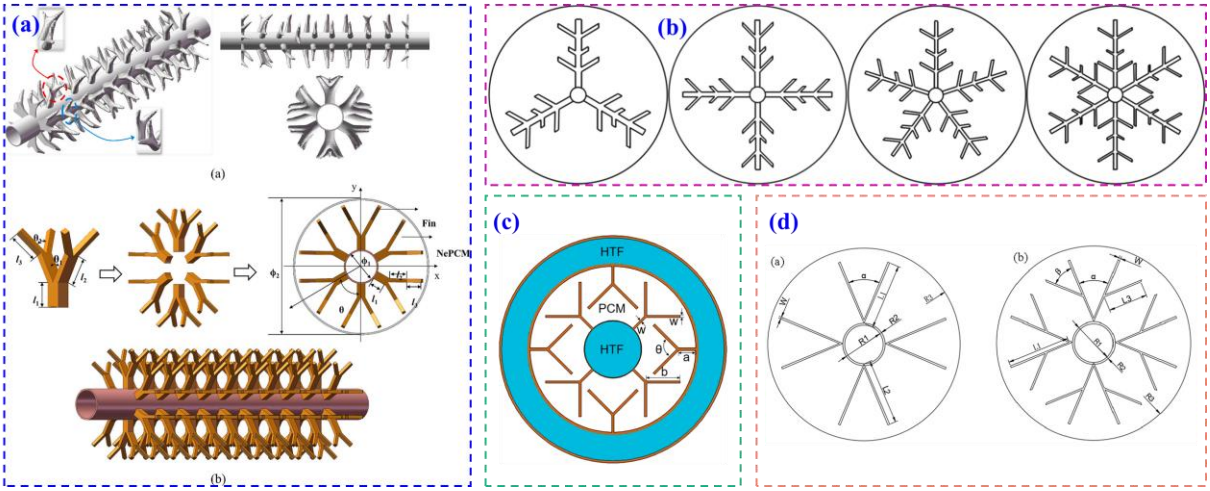

Fig. 14. Fin branch structure, (a) anisotropic fractal fin [129], (b) non-uniform Y-shaped fractal fin [130], (c) Y-shaped fin structure [132], (d) V-shaped fin [133].

4.4 Biomimetic structure

Researchers drew inspiration from biological structures in nature and discovered that biomimetic structures can effectively enhance efficiency. In the study of pipeline shape, Gao et al. [135] proposed a lotus root type thermal storage device (see Fig. 15(a)), which reduced the total melting time by 89.1% and increased the average temperature by 13.2 ℃ compared to traditional shell and tube thermal storage devices. Zhang et al. [136] experimentally studied the effect of biomimetic snowflake shaped fins (see Fig. 15(b)) on the energy storage/release performance of LHTES devices. They found that snowflake fins can shorten the melting/solidification time by 32%-52%, increase the average heat transfer rate by nearly 2 times during discharge and improve the charging and discharging efficiency by 51% and 25%, respectively. Qasem et al. [137] investigated octagonal shell-and-tube heat storage devices featuring straight double-radial fins, tree-like fins and root-like fin distributions, as illustrated

765 in Fig. 15(c). Their results demonstrated that root-like fins could significantly reduce heat
766 storage time by over 56%. Wang et al. [138] designed a perforated tree-like fin structure and
767 conducted numerical simulations to investigate the impact of the perforated layer on the overall
768 performance of the device. The study revealed that the three-layer perforated structure showed
769 the greatest improvement, with the number of holes having a more significant effect on heat
770 transfer than the hole diameter. Perforations enhanced natural convection during the initial
771 solidification stage. Yan et al. [139] investigated the effects of different structures and
772 arrangements of novel leaf-vein-inspired fins (see Fig. 15(d)) on the complete melting time of
773 PCM. Their results demonstrated that the novel fins could significantly shorten the complete
774 melting time. Altering the number of fin branches could save up to 16.9% of the melting time,
775 while increasing the fin angle could reduce the total melting time by up to 14.3%. Li et al. [140]
776 conducted a numerical study on the PCM melting performance in leaf-shaped longitudinal fin
777 assemblies with different structures. The results indicated that the total melting time for fins
778 with a triangular branching structure could be reduced by 30.1%. Zhang et al. [141] designed a
779 harpoon-shaped fin and found that longitudinal extension is more critical than horizontal
780 extension. The results showed that the heat transfer efficiency of the optimized fin structure was
781 6 times than finless structure and the total melting time was shortened by 85.9%. Moreover,
782 incorporating topology optimization techniques with the evolutionary processes of natural plant
783 structures, Liu et al. [142] proposed vertically arranged ring-shaped fins through biomimetic
784 topology optimization to accelerate heat storage performance. Experimental measurements
785 confirmed that the optimized biomimetic fins reduced melting time by 45.9% compared to

conventional fins. Huang et al. [143] employed biomimetic techniques to design an innovative heat accumulator featuring palmate-shaped fins. Research demonstrated that the charging and discharging times of the palmate-shaped fin heat storage device were reduced by 21.0% and 38.2%, respectively. Ren et al. [144] proposed a synergistic enhancement scheme combining bionic alveolar-like fins and pulsatile flow. Through numerical simulation and multi-objective optimization, they validated the effectiveness in improving PCM melting performance, achieving a 41.4% increase in melting efficiency.

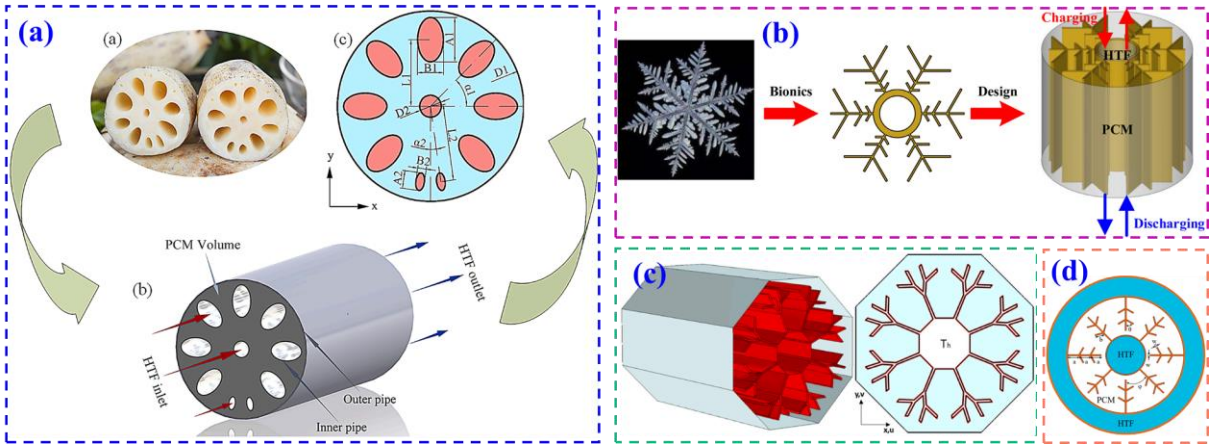

Fig. 15. (a) structure of the lotus-root [135], (b) snowflake shaped fins [136], (c) root-like fin [137], (d) leaf-vein-inspired fins [139].

4.5 Summary

In summary, factors such as the shape and number of inner tubes, fin structural parameters and arrangement configurations in phase change heat accumulators all affect their heat transfer efficiency and thermal storage performance. By rationally designing and optimizing these key parameters, the performance of such accumulators can be significantly improved, enhancing their suitability for engineering applications such as solar thermal energy storage.

The aforementioned studies indicated that structural optimization of heat accumulator can enhance the thermal storage and heat transfer performance to a certain extent. However, current research still faces several limitations. For example, existing topology optimization efforts have primarily focused on single-fin designs, lacking comprehensive optimization across multiple configurations. Additionally, the impact of reduced PCM volume due to fin insertion on the heat storage process has been neglected. Most studies have concentrated on the heat storage phase, while the thermal behavior during heat release and its correlation with structural parameters still require in-depth investigations. Future research should adopt multi-objective optimization strategies to balance heat transfer enhancement with the thermal storage capacity. Moreover, a comprehensive evaluation of thermal performance across the entire heat storage and release cycle is crucial for promoting the practical application of phase change thermal storage technologies.

5 Synergistic optimization of PCM and heat accumulator

Based on the findings of the aforementioned study, current research treats the optimization of PCM performance and the optimization of heat storage structure as two separate processes. Conventional PCM optimization typically focuses on improving thermal properties, such as phase change enthalpy, thermal conductivity, phase change temperature stability and cycle life. Whereas thermal storage structure optimization emphasizes enhancing heat transfer efficiency, optimizing flow field distribution, accelerating heat storage and release rates and improving structural compactness. Both types of optimization overlook the interdependent constraints between material properties and structural configuration, failing to leverage the performance

advantages of PCMs and heat accumulators simultaneously. This can even result in wasted material performance and low heat transfer efficiency. The synergistic optimization of PCMs and heat accumulators follows the principle of precision matching between performance and structure, with the ultimate optimization goals being the system's overall thermal storage density, heat transfer efficiency, cycle stability, and energy-saving benefits, achieving globally optimal performance. The synergistic design of PCMs and heat accumulators can significantly improve the overall thermal storage efficiency, shorten heat storage and release times, enhance internal temperature uniformity and prevent localized overheating issues [145]. Simultaneously, synergistic optimization can fully leverage the thermal storage potential of PCMs [146]. For the same thermal storage requirements, it reduces the need of PCMs, increasing the compactness and cost-effectiveness of the thermal storage system. Furthermore, a well-designed synergistic approach can enhance the structural stability and service life of the thermal storage unit, mitigating issues such as performance degradation, leakage, and failure of the PCMs caused by structural design flaws, advancing the application of phase-change energy storage technology in solar power generation.

6 Conclusions and perspectives

Thermal storage materials and heat accumulators are equally vital components in thermal storage systems. Based on a systematic analysis of the literature, the current state of research on nitrate-based PCMs and casing heat accumulators can be summarized as follows:

(1) Nitrate-based PCMs offer high thermal storage density and excellent thermal stability, making them suitable for direct application in medium-to-high temperature thermal storage

scenarios such as solar thermal power generation. Nitrate-based PCM mixtures are composed of proportionally blended nitrates, allowing flexible adjustment of phase transition temperatures to suit diverse scenarios between 100 ℃-500 ℃. However, precise control of component ratios is essential to prevent phase separation, corrosion, and thermal decomposition during prolonged high-temperature operation.

(2) Carbon-based materials significantly enhance the thermal conductivity of nitrate PCMs by constructing highly thermally conductive three-dimensional networks, addressing the core bottleneck of inefficient heat storage and release. Nanoparticles act as nucleating agents, effectively suppressing supercooling phenomena to ensure reliable solidification and heat release at set temperatures. Microencapsulation technology encapsulates the PCMs within micron-scale capsules, fundamentally preventing leakage during the molten state while enhancing cycle stability.

(3) Structural and design optimizations of heat accumulators play a pivotal role in maximizing thermal performance. Tube arrangement optimization improves the interaction between PCM and heat transfer fluid (HTF), reducing thermal resistance and accelerating melting. Fins increase effective heat transfer area, while topology optimization algorithms identify highly efficient non-uniform heat distribution patterns within constrained spaces. Bionic-inspired designs further enhance synergistic heat transfer effects by mimicking natural structures. Together, these strategies optimize conduction, convection and phase change processes, substantially enhancing heat storage/release efficiency and temperature stability of phase change heat accumulators.

Future efforts in nitrate-based phase change materials should focus on achieving precise control over phase change temperatures, enhancing thermal cycling stability, and expanding operational temperature ranges. By systematically tuning the composition ratios of multi-component nitrates, it is possible to develop PCMs with lower melting points, higher latent heat capacities, reduced corrosivity, and improved decomposition thresholds. Beyond single-component systems, composite designs that integrate functional materials with nitrates hold promise for simultaneously improving thermal storage density, material reliability, and overall system performance. The adoption of data-driven approaches, such as machine learning algorithms and artificial neural networks, can further accelerate the predictive design and optimization of high performance composite PCMs, providing a robust foundation for next-generation solar thermal applications. In parallel, the thermophysical properties of molten salts can be substantially enhanced through advanced additive technologies. While existing research primarily addresses single or dual-component nanoparticles, future work should explore synergistic multi-component systems, including combinations of carbon-based 2D materials such as MXene or g-C_3N_4 with metal oxides. Comprehensive investigations into the long-term cycling stability, thermal conductivity improvements, and economic feasibility of these modified molten salts are essential to enable large-scale deployment in concentrated solar power systems. Last but not at least, structural innovation and computational optimization remain key to maximizing the efficiency of phase change heat accumulators. Rational tube arrangements combined with fin structures can form highly effective heat transfer networks, while topology optimization techniques enable the identification of optimal material

distributions that balance thermal performance with structural efficiency. Incorporating biomimetic design principles, inspired by naturally efficient heat transfer systems, offers additional opportunities to create components that simultaneously exhibit superior thermal conductivity and mechanical stability. Together, these strategies provide a pathway to next-generation heat accumulators with enhanced energy utilization, rapid response rates, and improved operational reliability, supporting the advancement of high performance solar thermal energy storage systems.

Declaration of Competing Interest

The authors declared that there is no conflict of interest, and manuscript is approved by all authors for publication.

Acknowledgements

This work was financially supported by the Henan Key Research and Development Program (Grant No. 241111320900), the Postdoctoral Fellowship Program of CPSF (Grant No. GZC20250611), Key projects of Science and Technology of Henan Province (Grant No. 252102241001), the Key Research Project of Higher Education Department of Henan Province (Grant No. 26A470017), Doctoral Research Fund of Zhengzhou University of Light Industry (Grant No. NYY20250018).

References

[1] M.A. Khadimallah, A. Alanazi, M. Alanazi, et al., Simultaneous power, fresh water and fuel generation using a novel hybrid system based on biomass and solar thermal energy, Int. J.

Hydrogen. Energ. 70 (2024) 414-428, https://doi.org/10.1016/j.ijhydene.2024.05.210.

[2] P. Zhang, Q. Liao, H. Yao, et al., Direct solar steam generation system for clean water production, Energy. Storage. Mater. 18 (2019) 429-446, https://doi.org/10.1016/j.ensm.2018.10.006.

[3] Y. Qian, Z. Xu, Y. Qin, et al., A critical review on the multidimensional complexity of sustainable energy development, Appl. Energ. 394 (2025) 126194, https://doi.org/10.1016/j.apenergy.2025.126194.

[4] X. Ju, C. Xu, Y. Hu, et al., A review on the development of photovoltaic/concentrated solar power (PV-CSP) hybrid systems, Sol. Energ. Mat. Sol. C. 161 (2017) 305-327, https://doi.org/10.1016/j.solmat.2016.12.004.

[5] M. He, D. Sun, P. Wen, et al., Environmental control for Chinese solar greenhouses: A review, Renew. Sust. Energ. Rev. 218 (2025) 115796, https://doi.org/10.1016/j.rser.2025.115796.

[6] N. Campion, R. Gutiérrez-Alvarez, J.T.F. Bruce, et al., The potential role of concentrated solar power for off-grid green hydrogen and ammonia production, Renew. Energ. 236 (2024) 121410, https://doi.org/10.1016/j.renene.2024.121410.

[7] L. Heller, S. Glos, R. Buck, Cost benefit analysis of supercritical CO_2 cycles in next-generation solar thermal power plants, Renew. Energ. 256 (2026) 123613, https://doi.org/10.1016/j.renene.2025.123613.

[8] Z. Haddad, B. Buonomo, E. Abu-Nada, et al., A comprehensive review on the properties of micro/nano-encapsulated phase change materials: Single- to multi-layered shells, Renew. Sust. Energ. Rev. 205 (2024) 114826, https://doi.org/10.1016/j.rser.2024.114826.

[9] S. Mao, Y. Liu, X. Wu, et al., Thermal energy storage performance, application and challenge of phase change materials: a review, Energy Storage and Saving. 4 (2025) 300-322, https://doi.org/10.1016/j.enss.2025.03.001.

[10] H. Wang, J. Liu, Y. Wang, et al., A review of the performance and application of molten salt-based phase change materials in sustainable thermal energy storage at medium and high temperatures, Appl. Energ. 389 (2025) 125766, https://doi.org/10.1016/j.apenergy.2025.125766.

[11] M.A. Khaliquzzama, S.U. Masuri, R. Saidur, et al., Heat transfer analysis of molten salt nitrates inside shell and tube heat exchanger with small round holed segmental baffles for concentrated solar power, Int. J. Heat. Fluid. Fl. 116 (2025) 109916, https://doi.org/10.1016/j.ijheatfluidflow.2025.109916.

[12] D. Pardillos Pobo, P.A. González Gómez, M. Laporte Azcué, et al., Design of coil-wound heat exchangers for molten chloride salt TES in CSP with sodium receiver and sCO_2 cycle, J. Energy. Storage. 128 (2025) 117210, https://doi.org/10.1016/j.est.2025.117210.

[13] Z. Li, Y. Lu, R. Huang, et al., Applications and technological challenges for heat recovery, storage and utilisation with latent thermal energy storage, Appl. Energ. 283 (2021) 116277, https://doi.org/10.1016/j.apenergy.2020.116277.

[14] L. Chen, Y. Li, H. Fei, et al., Properties regulation and application of biomass carbon based composite phase change materials in thermal energy storage, Sol. Energy. 298 (2025) 113680, https://doi.org/10.1016/j.solener.2025.113680.

[15] G. Sadeghi, Energy storage on demand: Thermal energy storage development, materials, design, and integration challenges, Energy. Storage. Mater. 46 (2022) 192-222, https://doi.org/10.1016/j.ensm.2022.01.017.

[16] A. Gharehghani, M. Rabiei, S. Mehranfar, et al., Progress in battery thermal management systems technologies for electric vehicles, Renew. Sust. Energ. Rev. 202 (2024) 114654, https://doi.org/10.1016/j.rser.2024.114654.

[17] S. Zhang, Y. Yan, Energy, exergy and economic analysis of ceramic foam-enhanced molten salt as phase change material for medium- and high-temperature thermal energy storage, Energy. 262 (2023) 125462, https://doi.org/10.1016/j.energy.2022.125462.

[18] B. Németh, A. Ujhidy, J. Tóth, et al., Power consumption of model houses with and without PCM plaster lining using different heating methods, Energ. Buildings. 284 (2023) 112845, https://doi.org/10.1016/j.enbuild.2023.112845.

[19] G. Colelli, R. Chacartegui, C. Ortiz, et al., Life cycle and environmental assessment of calcium looping (CaL) in solar thermochemical energy storage, Energ. Convers. Manage. 257 (2022) 115428, https://doi.org/10.1016/j.enconman.2022.115428.

962 [20] A. Nur'aini, E. Laasonen, V. Ruuskanen, et al., Comparative analysis of molten salt
963 electrolytes for solid carbon production, Renew. Sust. Energ. Rev. 209 (2025) 115104,
964 https://doi.org/10.1016/j.rser.2024.115104.
965 [21] Q. Lin, Y. Xu, X. Yang, et al., Thermal stability and microstructure of sodium nitrite in
966 multicomponent molten salts: An experimental analysis, Sol. Energy. 283 (2024) 113008,
967 https://doi.org/10.1016/j.solener.2024.113008.
968 [22] Z. Qiao, H. Li, J. Wang, et al., Alkali-activated fly ash composite $NaNO_3$ thermal energy
969 storage materials: Low-temperature preparation and high-temperature stability, J. Energy.
970 Storage. 120 (2025) 116424, https://doi.org/10.1016/j.est.2025.116424.
971 [23] Y. Ren, C. Xu, M. Yuan, et al., $Ca(NO_3)_2$-$NaNO_3$/expanded graphite composite as a novel
972 shape-stable phase change material for mid- to high-temperature thermal energy storage, Energ.
973 Convers. Manage. 163 (2018) 50-58, https://doi.org/10.1016/j.enconman.2018.02.057.
974 [24] Y. Zhong, M. Wang, H. Wang, et al., Thermodynamic description of the quaternary
975 $Mg(NO_3)_2$–KNO_3–$NaNO_3$–$LiNO_3$ system and investigation on the novel $Mg(NO_3)_2$ based
976 nitrate salts with low temperature, Sol. Energ. Mat. Sol. C. 230 (2021) 111148,
977 https://doi.org/10.1016/j.solmat.2021.111148.
978 [25] R.I. Olivares, The thermal stability of molten nitrite/nitrates salt for solar thermal energy
979 storage in different atmospheres, Sol. Energy. 86 (2012) 2576-2583,
980 https://doi.org/10.1016/j.solener.2012.05.025.
981 [26] Z. Ma, J. Gifford, X. Wang, et al., Electric-thermal energy storage using solid particles as
982 storage media, Joule. 7 (2023) 843-848, https://doi.org/10.1016/j.joule.2023.03.016.
983 [27] R. Pérez-Álvarez, P.Á. González-Gómez, D. Santana, et al., Preheating of solar power
984 tower receiver tubes for a high-temperature chloride molten salt, Appl. Therm. Eng. 216 (2022)
985 119097, https://doi.org/10.1016/j.applthermaleng.2022.119097.
986 [28] P. Shi, B. Leng, X. Ye, et al., Tribological behavior of 316H stainless steel in $NaNO_3$-KNO_3
987 molten salt at elevated temperature, Sol. Energ. Mat. Sol. C. 257 (2023) 112377,
988 https://doi.org/10.1016/j.solmat.2023.112377.
989 [29] Y. Wang, Z. Wang, Y. Lu, et al., Phase diagram calculation and neural network prediction

of nitrate/nitrite molten salts with wide working temperature range for thermal storage system, Energy. 322 (2025) 135638, https://doi.org/10.1016/j.energy.2025.135638.

[30] H. Wang, J. Wei, L. Luo, et al., Thermophysical properties and phase diagram analysis of binary, ternary and quaternary nitrates for the thermal energy storage applications, Sol. Energy. 286 (2025) 113151, https://doi.org/10.1016/j.solener.2024.113151.

[31] H.A. Aljaerani, M. Samykano, A.K. Pandey, et al., Thermophysical properties enhancement and characterization of CuO nanoparticles enhanced HITEC molten salt for concentrated solar power applications, Int. Commun. Heat. Mass. 132 (2022) 105898, https://doi.org/10.1016/j.icheatmasstransfer.2022.105898.

[32] R.I. Olivares, W. Edwards, $LiNO_3$–$NaNO_3$–KNO_3 salt for thermal energy storage: Thermal stability evaluation in different atmospheres, Thermochimica Acta. 560 (2013) 34-42, https://doi.org/10.1016/j.tca.2013.02.029.

[33] Y. Wang, Y. Ma, Y. Lu, et al., Phase diagram thermodynamic calculation of KNO_3-$NaNO_2$-KNO_2 ternary system molten salt and its thermophysical properties investigation for thermal energy storage, J. Energy. Storage. 96 (2024) 112422, https://doi.org/10.1016/j.est.2024.112422.

[34] B. Li, X. Zhang, Y. Wang, et al., Thermophysical property degradation and structure evolution of the $NaNO_3$-KNO_3-$Ca(NO_3)_2$ molten salts after long-term high-temperature heat treatment, Sol. Energ. Mat. Sol. C. 290 (2025) 113668, https://doi.org/10.1016/j.solmat.2025.113668.

[35] C.Y. Zhao, Z.G. Wu, Thermal property characterization of a low melting-temperature ternary nitrate salt mixture for thermal energy storage systems, Sol. Energ. Mat. Sol. C. 95 (2011) 3341-3346, https://doi.org/10.1016/j.solmat.2011.07.029.

[36] M. Henríquez, L. Guerreiro, Á.G. Fernández, et al., Lithium nitrate purity influence assessment in ternary molten salts as thermal energy storage material for CSP plants, Renew. Energ. 149 (2020) 940-950, https://doi.org/10.1016/j.renene.2019.10.075.

[37] J. Wang, F. Xu, Y. Hu, et al., Thermodynamic investigation of the $Ca(NO_3)_2$–$NaNO_3$–KNO_3 system for solar thermal energy storage, Thermochimica Acta. 688 (2020) 178608, https://doi.org/10.1016/j.tca.2020.178608.

[38] A.G. Fernández, S. Ushak, H. Galleguillos, et al., Development of new molten salts with $LiNO_3$ and $Ca(NO_3)_2$ for energy storage in CSP plants, Appl. Energ. 119 (2014) 131-140, https://doi.org/10.1016/j.apenergy.2013.12.061.

[39] A.G. Fernandez, H. Galleguillos, E. Fuentealba, et al., Thermal characterization of HITEC molten salt for energy storage in solar linear concentrated technology, J. Therm. Anal. Calorim. 122 (2015) 3-9, https://doi.org/10.1007/s10973-015-4715-9.

[40] A.G. Fernández, S. Ushak, H. Galleguillos, et al., Thermal characterisation of an innovative quaternary molten nitrate mixture for energy storage in CSP plants, Sol. Energ. Mat. Sol. C. 132 (2015) 172-177, https://doi.org/10.1016/j.solmat.2014.08.020.

[41] A.M. Gasanaliev, B.Y. Gamataeva, Heat-accumulating properties of melts, Russ. Chem. Rev. 69 (2000) 192-200, https://doi.org/10.1070/RC2000v069n02ABEH000490.

[42] D. Mantha, T. Wang, R.G. Reddy, Thermodynamic modeling of eutectic point in the $LiNO_3$–$NaNO_3$–KNO_3–$NaNO_2$ quaternary system, Sol. Energ. Mat. Sol. C. 118 (2013) 18-21, https://doi.org/10.1016/j.solmat.2013.06.023.

[43] B.D. Iverson, S.T. Broome, A.M. Kruizenga, et al., Thermal and mechanical properties of nitrate thermal storage salts in the solid-phase, Sol. Energy. 86 (2012) 2897-2911, https://doi.org/10.1016/j.solener.2012.03.011.

[44] L.L. Zou, X. Chen, Y.T. Wu, et al., Experimental study of thermophysical properties and thermal stability of quaternary nitrate molten salts for thermal energy storage, Sol. Energ. Mat. Sol. C. 190 (2019) 12-19, https://doi.org/10.1016/j.solmat.2018.10.013.

[45] C.C. Kwasi-Effah, H.O. Egware, A.I. Obanor, et al., Development and characterization of a quaternary nitrate based molten salt heat transfer fluid for concentrated solar power plant, Heliyon. 9 (2023) e16096, https://doi.org/10.1016/j.heliyon.2023.e16096.

[46] D. Zhou, P. Eames, A study of a eutectic salt of lithium nitrate and sodium chloride (87–13%) for latent heat storage, Sol. Energ. Mat. Sol. C. 167 (2017) 157-161, https://doi.org/10.1016/j.solmat.2017.04.016.

[47] R. Kumar, A. Nirwan, A. Dixit, Enhanced thermal conductivity and shape stabilized $LiNO_3$-NaCl eutectic/exfoliated graphite composite for thermal energy storage applications,

Energy Storage. 4 (2022) e296, https://doi.org/10.1002/est2.296.

[48] L. Sang, X. Lv, Y. Wu, $NaNO_3$-KNO_3-KCl/K_2CO_3 with the elevated working temperature for CSP application: Phase diagram calculation and machine learning, Sol. Energy. 252 (2023) 322-329, https://doi.org/10.1016/j.solener.2023.02.009.

[49] Y. Li, Z. Fu, S. Zhou, et al., The thermal performance and corrosiveness of a new type of molten salt $LiNO_3$-KNO_3-KCl, Int. Commun. Heat. Mass. 162 (2025) 108600, https://doi.org/10.1016/j.icheatmasstransfer.2025.108600.

[50] Y. Li, S.H. Zhou, S.L. Jiang, et al., Preparation and thermal properties of $LiNO_3$-$NaNO_3$-NaCl/EG composite heat storage material, Sol. Energy. 263 (2023) 111926, https://doi.org/10.1016/j.solener.2023.111926.

[51] M. Castro-Quijada, D. Faundez, R. Rojas, et al., Improving the working fluid based on a $NaNO_3$-KNO_3-NaCl-KCl molten salt mixture for concentrating solar power energy storage, Sol. Energy. 231 (2022) 464-472, https://doi.org/10.1016/j.solener.2021.11.058.

[52] X. Lai, H. Yin, P. Li, et al., Design optimization and thermal storage characteristics of $NaNO_3$-NaCl-NaF molten salts with high latent heat and low cost for the thermal energy storage, J. Energy. Storage. 52 (2022) 104805, https://doi.org/10.1016/j.est.2022.104805.

[53] H. Na, C. Zhang, Y. Wu, et al., Investigation on thermal performance of eutectic binary nitrate-carbonate molten salt under thermal shock condition, Sol. Energ. Mat. Sol. C. 255 (2023) 112314, https://doi.org/10.1016/j.solmat.2023.112314.

[54] H. Na, C. Zhang, Y. Wu, et al., Effect of Na_2CO_3 content on thermophysical properties, corrosion behaviors of KNO_3-$NaNO_2$ molten salt, Energy. 311 (2024) 133378, https://doi.org/10.1016/j.energy.2024.133378.

[55] L. Sang, X. Lv, Y. Wang, et al., Investigation of KNO_2-KNO_3-K_2CO_3 mixed molten salts with higher working temperature for supercritical CO_2 concentrated solar power application, J. Energy. Storage. 61 (2023) 106724, https://doi.org/10.1016/j.est.2023.106724.

[56] H. Huang, W. Liu, B. Li, et al., Design and key thermo-physical properties of $NaNO_3$-KNO_3-Na_2CO_3-NaCl with high thermal stability for thermal energy storage, Sol. Energ. Mat. Sol. C. 283 (2025) 113459, https://doi.org/10.1016/j.solmat.2025.113459.

[57] Á.G. Fernández, L.F. Cabeza, Molten salt corrosion mechanisms of nitrate based thermal energy storage materials for concentrated solar power plants: A review, Sol. Energ. Mat. Sol. C. 194 (2019) 160-165, https://doi.org/10.1016/j.solmat.2019.02.012.

[58] A.G. Fernández, H. Galleguillos, F.J. Pérez, Thermal influence in corrosion properties of Chilean solar nitrates, Sol. Energy. 109 (2014) 125-134, https://doi.org/10.1016/j.solener.2014.07.027.

[59] G. McConohy, A. Kruizenga, Molten nitrate salts at 600 and 680°C: Thermophysical property changes and corrosion of high-temperature nickel alloys, Sol. Energy. 103 (2014) 242-252, https://doi.org/10.1016/j.solener.2014.01.028.

[60] M. Lague, A. Sagade, S. Leiva-Guajardo, et al., Short overview of flow-accelerated corrosion in CSP systems using molten nitrate salts: Mechanisms, challenges and outlook, Sol. Energy. 303 (2026) 114116, https://doi.org/10.1016/j.solener.2025.114116.

[61] N. Ren, Y.T. Wu, C.F. Ma, et al., Preparation and thermal properties of quaternary mixed nitrate with low melting point, Sol. Energ. Mat. Sol. C. 127 (2014) 6-13, https://doi.org/10.1016/j.solmat.2014.03.056.

[62] C.C. Kwasi-Effah, O. Ighodaro, H.O. Egware, et al., Characterization and comparison of the thermophysical property of ternary and quaternary salt mixtures for solar thermal power plant applications, Results. Eng. 16 (2022) 100721, https://doi.org/10.1016/j.rineng.2022.100721.

[63] X. Li, Y. Wang, S. Wu, et al., Preparation and investigation of multicomponent alkali nitrate/nitrite salts for low temperature thermal energy storage, Energy. 160 (2018) 1021-1029, https://doi.org/10.1016/j.energy.2018.07.078.

[64] X.Y. Zhang, Y.T. Ge, Burra, et al., Experimental investigation and CFD modelling analysis of finned-tube PCM heat exchanger for space heating, Appl. Therm. Eng. 244 (2024) 122731, https://doi.org/10.1016/j.applthermaleng.2024.122731.

[65] X.H. Wu, Y.N. Chen, J.W. Hou, et al., Performance characterization of form-stable carbon-based network microcapsules for thermal energy storage, Appl. Therm. Eng. 212 (2022) 118632, https://doi.org/10.1016/j.applthermaleng.2022.118632.

[66] H. Waqas, M.J. Hasan, C. Ji, et al., Melting performance of PCM with MoS_2 and Fe_3O_4 nanoparticles using leaf-based fins with different orientations in a shell and tube-based TES system, Int. Commun. Heat. Mass. 158 (2024) 107944, https://doi.org/10.1016/j.icheatmasstransfer.2024.107944.

[67] X. Wu, M. Gao, K. Wang, et al., Experimental study of the thermal properties of a homogeneous dispersion system of a paraffin-based composite phase change materials, J. Energy. Storage. 36 (2021) 102398, https://doi.org/10.1016/j.est.2021.102398.

[68] Y. Yu, Y. Tao, C. Zhao, et al., Thermal storage performance enhancement and regulation mechanism of KNO_3-SWCNT based composite phase change materials, Int. J. Heat. Mass. Tran. 181 (2021) 121870, https://doi.org/10.1016/j.ijheatmasstransfer.2021.121870.

[69] Y. Wu, J. Li, M. Wang, et al., Solar salt doped by MWCNTs as a promising high thermal conductivity material for CSP, RSC Advances. 8 (2018) 19251-19260, https://doi.org/10.1039/C8RA03019G.

[70] H. Lyu, D. Feng, Y. Feng, et al., Enhanced thermal energy storage of sodium nitrate by graphene nanosheets: Experimental study and mechanisms, J. Energy. Storage. 54 (2022) 105294, https://doi.org/10.1016/j.est.2022.105294.

[71] X. Wu, K. Hao, M. Zhao, et al., Investigation on thermal property enhancement of low melting point ternary molten salt and composite materials, Int. Commun. Heat. Mass. 169 (2025) 109332, https://doi.org/10.1016/j.icheatmasstransfer.2025.109332.

[72] Q. Zhu, P.J. Ong, S.H.A. Goh, et al., Recent advances in graphene-based phase change composites for thermal energy storage and management, Nano Materials Science. 6 (2024) 115-138, https://doi.org/10.1016/j.nanoms.2023.09.003.

[73] H. Lei, X. Wang, Y. Li, et al., Organic-inorganic hybrid phase change materials with high energy storage density based on porous shaped paraffin/hydrated salt/expanded graphite composites, Energy. 304 (2024) 132169, https://doi.org/10.1016/j.energy.2024.132169.

[74] Y. Li, W.C. Tie, Q.Z. Zhu, et al., A study of $LiNO_3$-NaCl/EG composite PCM for latent heat storage, Int. J. Thermophys. 42 (2021) 1-11, https://doi.org/10.1007/s10765-021-02908-8.

[75] Y. Li, S.H. Zhou, S. Wang, et al., Preparation and thermal properties of a novel ternary

molten salt/expanded graphite thermal storage material, J. Energy. Storage. 74 (2023) 109273, https://doi.org/10.1016/j.est.2023.109273.

[76] Y. Li, G. Yue, Y.M. Yu, et al., Preparation and thermal characterization of $LiNO_3$-$NaNO_3$-KCl ternary mixture and $LiNO_3$-$NaNO_3$-KCl/EG composites, Energy. 196 (2020) 117067, https://doi.org/10.1016/j.energy.2020.117067.

[77] P.D. Myers, T.E. Alam, R. Kamal, et al., Nitrate salts doped with CuO nanoparticles for thermal energy storage with improved heat transfer, Appl. Energ. 165 (2016) 225-233, https://doi.org/10.1016/j.apenergy.2015.11.045.

[78] H.W. Son, C.S. Heu, H.S. Lee, et al., Enhanced thermal performance of lithium nitrate phase change material by porous copper oxide nanowires integrated on folded meshes for high temperature heat storage, Chem. Eng. J. 391 (2020) 123613, https://doi.org/10.1016/j.cej.2019.123613.

[79] A. Awad, H. Navarro, Y. Ding, et al., Thermal-physical properties of nanoparticle-seeded nitrate molten salts, Renew. Energ. 120 (2018) 275-288, https://doi.org/10.1016/j.renene.2017.12.026.

[80] Y. Hu, Z. Zhang, H. Gao, et al., Forced convective heat transfer of solar salt-based Al_2O_3 nanofluids using lattice Boltzmann method, Therm. Sci. Eng. Prog. 8 (2018) 2-9, https://doi.org/10.1016/j.tsep.2018.07.013.

[81] X. Wei, Y. Yin, B. Qin, et al., Preparation and enhanced thermal conductivity of molten salt nanofluids with nearly unaltered viscosity, Renew. Energ. 145 (2020) 2435-2444, https://doi.org/10.1016/j.renene.2019.04.153.

[82] L. Meng, C. Zhang, Y. Wu, et al., Study on thermophysical properties improvement of ternary nitrate-carbonate molten salt by adding SiO_2 nanoparticles for large-scale thermal energy storage, Sol. Energ. Mat. Sol. C. 292 (2025) 113819, https://doi.org/10.1016/j.solmat.2025.113819.

[83] S. Jeong, B. Jo, Distinct behaviors of KNO_3 and $NaNO_3$ in specific heat enhancement of molten salt nanofluid, J. Energy. Storage. 57 (2023) 106209, https://doi.org/10.1016/j.est.2022.106209.

[84] B. El Far, S.M.M. Rizvi, Y. Nayfeh, et al., Study of viscosity and heat capacity characteristics of molten salt nanofluids for thermal energy storage, Sol. Energ. Mat. Sol. C. 210 (2020) 110503, https://doi.org/10.1016/j.solmat.2020.110503.

[85] B. Tian, C. Zhu, M. Gu, et al., Thermophysical properties enhancement of KNO_3–$NaNO_3$–$NaNO_2$ mixed with SiO_2/MgO nanoparticles, J. Sci-Adv. Mater. Dev. 10 (2025) 100849, https://doi.org/10.1016/j.jsamd.2025.100849.

[86] X. Xiao, H. Jia, D. Wen, et al., Experimental investigation of a latent heat thermal energy storage unit encapsulated with molten salt/metal foam composite seeded with nanoparticles, Energy. Built. Environ. 4 (2023) 74-85, https://doi.org/10.1016/j.enbenv.2021.08.003.

[87] W.P. Wong, R. Walvekar, M. Vaka, et al., Hybrid MWCNT/TiO_2 nanoparticles based high-temperature quinary nitrate salt mixture for thermal energy storage applications, J. Energy. Storage. 73 (2023) 108792, https://doi.org/10.1016/j.est.2023.108792.

[88] Q. Yu, Y. Lu, X. Zhang, et al., Comprehensive thermal properties of molten salt nanocomposite materials base on mixed nitrate salts with SiO_2/TiO_2 nanoparticles for thermal energy storage, Sol. Energ. Mat. Sol. C. 230 (2021) 111215, https://doi.org/10.1016/j.solmat.2021.111215.

[89] Z. Chang, K. Wang, X. Wu, et al., Review on the preparation and performance of paraffin-based phase change microcapsules for heat storage, J. Energy. Storage. 46 (2022) 103840, https://doi.org/10.1016/j.est.2021.103840.

[90] S.A. Albdour, Z. Haddad, O.Z. Sharaf, et al., Micro/nano-encapsulated phase-change materials (ePCMs) for solar photothermal absorption and storage: Fundamentals, recent advances, and future directions, Prog. Energ. Combust. 93 (2022) 101037, https://doi.org/10.1016/j.pecs.2022.101037.

[91] S. Chen, X. Cheng, Y. Li, et al., Study on the microstructures and thermal properties of SiO_2@$NaNO_3$ microcapsule thermal storage materials, Int. J. Energ. Res. 44 (2020) 10008-10022, https://doi.org/10.1002/er.5566.

[92] J. Lee, B. Jo, Nanoencapsulation of binary nitrate molten salts for thermal energy storage: Synthesis, thermal performance, and thermal reliability, Sol. Energ. Mat. Sol. C. 230 (2021)

111284, https://doi.org/10.1016/j.solmat.2021.111284.
[93] W. Ji, X. Cheng, H. Chen, et al., Efficient synthesis of regular spherical GO/SiO_2@Solar Salt microcapsules to enhance heat-storage capacity and cycle stability, Energ. Convers. Manage. 245 (2021) 114637, https://doi.org/10.1016/j.enconman.2021.114637.
[94] U. Nithiyanantham, A. Zaki, Y. Grosu, et al., SiO2@Al2O3 core-shell nanoparticles based molten salts nanofluids for thermal energy storage applications, J. Energy. Storage. 26 (2019) 101033, https://doi.org/10.1016/j.est.2019.101033.
[95] L. Wang, Y. Huang, L. Li, et al., Binary nitrate molten salt magnetic microcapsules modified with Fe_3O_4-functionalized carbon nanotubes for accelerating thermal energy storage, J. Energy. Storage. 74 (2023) 109394, https://doi.org/10.1016/j.est.2023.109394.
[96] T. Xiao, J. Xu, J. Xie, et al., Advanced encapsulation strategies for high-temperature molten salt: Synthesis methods and performance enhancement, Renew. Sust. Energ. Rev. 218 (2025) 115818, https://doi.org/10.1016/j.rser.2025.115818.
[97] Y. Ren, C. Xu, Q. Zhang, et al., Progress in optimizing thermal performance of nitrate salts and their mixtures for thermal energy storage, Renew. Sust. Energ. Rev. 212 (2025) 115379, https://doi.org/10.1016/j.rser.2025.115379.
[98] C. Wang, S. Wang, X. Cheng, et al., Research progress and performance improvement of phase change heat accumulators, J. Energy. Storage. 56 (2022) 105884, https://doi.org/10.1016/j.est.2022.105884.
[99] Q. Mao, Y. Zhao, Thermal storage performance of a horizontal eccentric distance spiral shell-tube heat storage tank, Appl. Therm. Eng. 236 (2024) 121818, https://doi.org/10.1016/j.applthermaleng.2023.121818.
[100] H. Zheng, D. Fu, C. Zhang, et al., Investigation on heat transfer characteristic of nitrate/nitrite molten salt nanofluids in bidirectional twisted tube, Therm. Sci. Eng. Prog. 57 (2025) 103194, https://doi.org/10.1016/j.tsep.2024.103194.
[101] W. Ye, J.M. Khodadadi, Effects of varying geometrical parameters on the melting performance of phase change materials within L-shaped shell-and-tube latent heat thermal energy storage units with radial eccentricity exhibiting prominent influence, J. Energy. Storage.

86 (2024) 111334, https://doi.org/10.1016/j.est.2024.111334.
[102] X. Li, S. Chen, Y. Tan, et al., Thermal storage performance of a novel shell-and-tube latent heat storage system: Active role of inner tube improvement and fin distribution optimization, Renew. Energ. 228 (2024) 120695, https://doi.org/10.1016/j.renene.2024.120695.
[103] A.H. Eisapour, A.H. Shafaghat, H.I. Mohammed, et al., A new design to enhance the conductive and convective heat transfer of latent heat thermal energy storage units, Appl. Therm. Eng. 215 (2022) 118955, https://doi.org/10.1016/j.applthermaleng.2022.118955.
[104] F. Narges Moghadam, E. Izadpanah, Y. Shekari, et al., Experimental evaluation of shell geometry impact on thermal and exergy performance in helical coiled tube heat exchanger with phase change material, J. Energy. Storage. 83 (2024) 110790, https://doi.org/10.1016/j.est.2024.110790.
[105] N.B. Khedher, N. Biswas, H. Togun, et al., Geometry modification of a vertical shell-and-tube latent heat thermal energy storage system using a framed structure with different undulated shapes for the phase change material container during the melting process, J. Energy. Storage. 72 (2023) 108365, https://doi.org/10.1016/j.est.2023.108365.
[106] S. Deng, C. Nie, H. Jiang, et al., Evaluation and optimization of thermal performance for a finned double tube latent heat thermal energy storage, Int. J. Heat. Mass. Tran. 130 (2019) 532-544, https://doi.org/10.1016/j.ijheatmasstransfer.2018.10.126.
[107] X. Yang, Z. Lu, Q. Bai, et al., Thermal performance of a shell-and-tube latent heat thermal energy storage unit: Role of annular fins, Appl. Energ. 202 (2017) 558-570, https://doi.org/10.1016/j.apenergy.2017.05.007.
[108] X. Wu, K. Hao, Z. Chang, et al., Study on temperature distribution optimization and enhanced heat transfer in shell and tube phase change accumulator, Renew. Energ. 242 (2025) 122469, https://doi.org/10.1016/j.renene.2025.122469.
[109] J.M. Mahdi, S. Lohrasbi, D.D. Ganji, et al., Accelerated melting of PCM in energy storage systems via novel configuration of fins in the triplex-tube heat exchanger, Int. J. Heat. Mass. Tran. 124 (2018) 663-676, https://doi.org/10.1016/j.ijheatmasstransfer.2018.03.095.
[110] F.L. Rashid, A.F. Khalaf, A.a. Alizadeh, et al., Numerical investigation of the effect of the

1242 number of fins on the phase-change material melting inside a shell-and-tube cylindrical thermal
1243 energy storage, Case. Stud. Therm. Eng. 60 (2024) 104754,
1244 https://doi.org/10.1016/j.csite.2024.104754.
1245 [111] A. Tavakoli, M. Farzaneh-Gord, A. Ebrahimi-Moghadam, Using internal sinusoidal fins
1246 and phase change material for performance enhancement of thermal energy storage systems:
1247 Heat transfer and entropy generation analyses, Renew. Energ. 205 (2023) 222-237,
1248 https://doi.org/10.1016/j.renene.2023.01.074.
1249 [112] S. Agrawal, P.M. Sutheesh, L.G. Kirankumar, et al., Numerical investigations on thermal
1250 performance of latent heat thermal energy storage system with novel corrugated annular fins in
1251 PCM, J. Energy. Storage. 125 (2025) 116902, https://doi.org/10.1016/j.est.2025.116902.
1252 [113] K.R. V, B. V, Enhancing thermal performance of latent heat storage unit for solar cooling:
1253 A hybrid approach with C-shaped fins and nano-additives, Appl. Energ. 351 (2023) 121825,
1254 https://doi.org/10.1016/j.apenergy.2023.121825.
1255 [114] J. Wang, S.A. Khan, M. Imran, et al., Computational investigation of melting performance
1256 enhancement in PCM-based lobed triplex-tube heat exchangers with Y-shaped fins for solar
1257 thermal energy storage, Int. Commun. Heat. Mass. 169 (2025) 109567,
1258 https://doi.org/10.1016/j.icheatmasstransfer.2025.109567.
1259 [115] L. Wang, Y. Lei, B. Du, et al., Performance enhancement of a horizontal latent thermal
1260 energy storage unit with elliptical fins, Appl. Therm. Eng. 225 (2023) 120191,
1261 https://doi.org/10.1016/j.applthermaleng.2023.120191.
1262 [116] J. Wołoszyn, K. Szopa, A combined heat transfer enhancement technique for shell-and-
1263 tube latent heat thermal energy storage, Renew. Energ. 202 (2023) 1342-1356,
1264 https://doi.org/10.1016/j.renene.2022.12.010.
1265 [117] J. Guo, Z. Liu, B. Yang, et al., Melting assessment on the angled fin design for a novel
1266 latent heat thermal energy storage tube, Renew. Energ. 183 (2022) 406-422,
1267 https://doi.org/10.1016/j.renene.2021.11.007.
1268 [118] N. Zhang, X. Cao, X. Fan, et al., Thermal storage performance of latent heat thermal
1269 energy storage device with helical fin under realistic working conditions, Appl. Therm. Eng.

236 (2024) 121668, https://doi.org/10.1016/j.applthermaleng.2023.121668.
[119] L. Lv, Y. Zou, S. Huang, et al., Experimental study on a pilot-scale medium-temperature latent heat storage system with various fins, Renew. Energ. 205 (2023) 499-508, https://doi.org/10.1016/j.renene.2023.01.089.
[120] Y.K. Liu, Y.B. Tao, Experimental and numerical investigation of longitudinal and annular finned latent heat thermal energy storage unit, Sol. Energy. 243 (2022) 410-420, https://doi.org/10.1016/j.solener.2022.08.023.
[121] S. Tang, Y. Song, P. Liu, et al., Experimental study on melting performance and uniformity of thermal energy storage systems with discontinuous fins, Appl. Therm. Eng. 278 (2025) 127429, https://doi.org/10.1016/j.applthermaleng.2025.127429.
[122] M. Izadi, I. Pop, S.A. Shehzad, et al., Comprehensive review of optimization strategies for phase change materials: Techniques, applications, and challenges in thermal storage systems, Int. Commun. Heat. Mass. 166 (2025) 109123, https://doi.org/10.1016/j.icheatmasstransfer.2025.109123.
[123] S. Zhang, G. Favero, G. Slaviero, et al., Designing fin structure by topology optimization for maximizing heat transfer efficiency of latent thermal energy storage, Int. Commun. Heat. Mass. 165 (2025) 109000, https://doi.org/10.1016/j.icheatmasstransfer.2025.109000.
[124] I.A. Laasri, Z. Elmaazouzi, A. Outzourhit, et al., Investigation of different topology-optimized fin structures in a cylindrical latent heat thermal energy storage unit, Therm. Sci. Eng. Prog. 33 (2022) 101372, https://doi.org/10.1016/j.tsep.2022.101372.
[125] R. Ge, G. Humbert, R. Martinez, et al., Additive manufacturing of a topology-optimised multi-tube energy storage device: Experimental tests and numerical analysis, Appl. Therm. Eng. 180 (2020) 115878, https://doi.org/10.1016/j.applthermaleng.2020.115878.
[126] Y. Chen, Y. Liu, H. Que, et al., Analysis on the effect of novel topological optimization fin structures considering eccentricity on the heat storage and release characteristics of shell and tube phase change heat accumulator, J. Energy. Storage. 97 (2024) 112880, https://doi.org/10.1016/j.est.2024.112880.
[127] X. Zhang, X. Yang, X. Gao, et al., Heat transfer characteristics of topological latent heat

storage systems based on optimization objectives, Appl. Therm. Eng. 252 (2024) 123674, https://doi.org/10.1016/j.applthermaleng.2024.123674.

[128] Z. He, H. Ma, S. Lu, Design and experimental investigation of topology-optimized fin structures for enhanced heat transfer in latent heat thermal energy storage units, J. Energy. Storage. 80 (2024) 110272, https://doi.org/10.1016/j.est.2023.110272.

[129] Z. Song, J. Wang, S. Tang, et al., Design and optimization of 3D anisotropic fractal fin structures for efficient latent heat storage systems, Int. Commun. Heat. Mass. 169 (2025) 109528, https://doi.org/10.1016/j.icheatmasstransfer.2025.109528.

[130] W. Li, J. Wang, Y. Zhang, et al., Numerical study and parametric analysis on performance enhancement of a latent heat storage unit with fractal fins, J. Energy. Storage. 55 (2022) 105814, https://doi.org/10.1016/j.est.2022.105814.

[131] Z. Liu, Z. Liu, G. Liu, et al., Melting assessment on the effect of nonuniform Y-shaped fin upon solid–liquid phase change in a thermal storage tank, Appl. Energ. 321 (2022) 119330, https://doi.org/10.1016/j.apenergy.2022.119330.

[132] P. Yan, W. Fan, Y. Yang, et al., Performance enhancement of phase change materials in triplex-tube latent heat energy storage system using novel fin configurations, Appl. Energ. 327 (2022) 120064, https://doi.org/10.1016/j.apenergy.2022.120064.

[133] C. Ao, S. Yan, W. Hu, et al., Heat transfer analysis of a PCM in shell-and-tube thermal energy storage unit with different V-shaped fin structures, Appl. Therm. Eng. 216 (2022) 119079, https://doi.org/10.1016/j.applthermaleng.2022.119079.

[134] S. Yao, M. Zuo, X. Huang, Evaluation and optimization of the thermal storage performance of a triplex-tube thermal energy storage system with V-shaped fins, J. Therm. Sci. 32 (2023) 2048-2064, https://doi.org/10.1007/s11630-023-1795-x.

[135] L. Gao, Y. Deng, S. Liu, et al., Design and optimization of a bionic-lotus root inspired shell-and-tube latent heat thermal energy storage unit, Int. J. Heat. Mass. Tran. 226 (2024) 125437, https://doi.org/10.1016/j.ijheatmasstransfer.2024.125437.

[136] Y. Zhang, B. Lu, Z. Wang, et al., Experimental investigation on the charging and discharging performance enhancement of a vertical latent heat thermal energy storage unit via

snowflake fin design, Int. J. Heat. Mass. Tran. 199 (2022) 123455, https://doi.org/10.1016/j.ijheatmasstransfer.2022.123455.

[137] N.A.A. Qasem, A. Belazreg, Y. Khetib, et al., Effect of novel fin distribution on the melting process of thermal storage units, Appl. Therm. Eng. 243 (2024) 122547, https://doi.org/10.1016/j.applthermaleng.2024.122547.

[138] Z. Wang, Y. Wang, L. Yang, et al., Multi-objective optimization of heat charging performance of phase change materials in tree-shaped perforated fin heat exchangers, Energy. 294 (2024) 130839, https://doi.org/10.1016/j.energy.2024.130839.

[139] P. Yan, W. Fan, Y. Han, et al., Leaf-vein bionic fin configurations for enhanced thermal energy storage performance of phase change materials in smart heating and cooling systems, Appl. Energ. 346 (2023) 121352, https://doi.org/10.1016/j.apenergy.2023.121352.

[140] C. Li, Q. Li, R. Ge, Assessment on the melting performance of a phase change material based shell and tube thermal energy storage device containing leaf-shaped longitudinal fins, J. Energy. Storage. 60 (2023) 106574, https://doi.org/10.1016/j.est.2022.106574.

[141] J. Zhang, S. Wen, S. Liu, et al., Numerical study on melting process and heat transfer analysis of a multitube combination latent heat storage unit with innovative harpoon-type fins, Appl. Therm. Eng. 233 (2023) 121168, https://doi.org/10.1016/j.applthermaleng.2023.121168.

[142] X. Liu, X. Qin, Y. Tian, et al., Biomimetic optimized vertically aligned annular fins for fast latent heat thermal energy storage, Appl. Energ. 347 (2023) 121435, https://doi.org/10.1016/j.apenergy.2023.121435.

[143] Y. Huang, Z. Deng, Y. Chen, et al., Performance investigation of a biomimetic latent heat thermal energy storage device for waste heat recovery in data centers, Appl. Energ. 335 (2023) 120745, https://doi.org/10.1016/j.apenergy.2023.120745.

[144] F. Ren, Q. Li, L. Shi, et al., Enhanced thermal performance of latent heat thermal energy storage systems with pulsating flow: A biomimetic approach inspired by alveolar vascular structures, Renew. Energ. 251 (2025) 123417, https://doi.org/10.1016/j.renene.2025.123417.

[145] Y.X. Chen, Y. Liu, L. Zeng, et al., A novel topology optimization of fin structure in shell-tube phase change accumulator considering the double objective functions and natural

convection, J. Energy. Storage. 80 (2024) 110327, https://doi.org/10.1016/j.est.2023.110327.

[146] G. Tanda, C. Champ, S. Barberis, Thermal optimization of a PCM-based heat exchanger: A modeling approach, Appl. Therm. Eng. 280 (2025) 128271, https://doi.org/10.1016/j.applthermaleng.2025.128271.